AD_____

AWARD NUMBER: DAMD17-03-1-0297

TITLE: Genomic and Expression Profiling of Benign & Malignant Nerve Sheath Tumors in Neurofibromatosis Patients

PRINCIPAL INVESTIGATOR: Matt van de Rijn, M.D., Ph.D.
Torsten Nielsen, M.D., Ph.D.
Brian Rubin, M.D., Ph.D.

CONTRACTING ORGANIZATION: Leland Stanford Junior University
Stanford, California 94305-4125

REPORT DATE: May 2006

TYPE OF REPORT: Annual

PREPARED FOR: U.S. Army Medical Research and Materiel Command
Fort Detrick, Maryland 21702-5012

REPORT DOCUMENTATION PAGE

Form Approved
OMB No. 0704-0188

1. REPORT DATE *(DD-MM-YYYY)*	**2. REPORT TYPE**	**3. DATES COVERED** *(From - To)*
01-05-2006	Annual	1 May 2005 – 30 Apr 2006

4. TITLE AND SUBTITLE

Genomic and Expression Profiling of Benign & Malignant Nerve Sheath Tumors in Neurofibromatosis Patients

5a. CONTRACT NUMBER

5b. GRANT NUMBER
DAMD17-03-1-0297

5c. PROGRAM ELEMENT NUMBER

6. AUTHOR(S)
Matt van de Rijn, M.D., Ph.D.; Torsten Nielsen, M.D., Ph.D. and
Brian Rubin, M.D., Ph.D.

E-Mail: mrijn@stanford.edu

5d. PROJECT NUMBER

5e. TASK NUMBER

5f. WORK UNIT NUMBER

7. PERFORMING ORGANIZATION NAME(S) AND ADDRESS(ES)

Leland Stanford Junior University
Stanford, California 94305-4125

8. PERFORMING ORGANIZATION REPORT NUMBER

9. SPONSORING / MONITORING AGENCY NAME(S) AND ADDRESS(ES)
U.S. Army Medical Research and Materiel Command
Fort Detrick, Maryland 21702-5012

10. SPONSOR/MONITOR'S ACRONYM(S)

11. SPONSOR/MONITOR'S REPORT NUMBER(S)

12. DISTRIBUTION / AVAILABILITY STATEMENT
Approved for Public Release; Distribution Unlimited

13. SUPPLEMENTARY NOTES

14. ABSTRACT

The goal of the study is to identify genes and pathways that are associated with the progression of neurofibroma to MPNST, and to identify potential therapeutic targets for MPNSTs. In the past year, to the existing 80 gene array data, we added an additional 23 tumor samples making to a total of 103 gene arrays. The analyses included 38 cases diagnosed as MPNSTs and 24 cases of neurofibromas. Our initial hierarchical clustering showed high degree of variability of MPNST cases. A centralized review of histology was performed; of the 38 cases with the original diagnosis as MPNST, 14 cases were reclassified. In addition all MPNST and SS cases underwent RT-PCR for t(X;18). The misdiagnosed tumor cases were removed from the study, and a subsequent analysis and hierarchical clustering showed a much more interpretable result. The clustering of the nerve sheath tumors revealed a distinct expression signature for majority of benign and malignant tumor types. A subset of MPNSTs clustered along with SS. Using a large tissue microarray (TMA) with about 200 nerve sheath tumors we have identified a novel diagnostic marker TLE1 to distinguish SS from other sarcomas. The signaling pathways TGFB, JAK- STAT, MET were identified as being potentially involved in the malignant transformation. Array comparative genomic hybridization was performed on 28 tumor cases and copy number changes were assessed for each case.

15. SUBJECT TERMS
gene microarrays, expression profiling, tissue microarrays, in situ hybridization

16. SECURITY CLASSIFICATION OF:			**17. LIMITATION OF ABSTRACT**	**18. NUMBER OF PAGES**	**19a. NAME OF RESPONSIBLE PERSON**
a. REPORT	**b. ABSTRACT**	**c. THIS PAGE**			USAMRMC
U	U	U	UU	55	**19b. TELEPHONE NUMBER** *(include area code)*

Standard Form 298 (Rev. 8-98)
Prescribed by ANSI Std. Z39.18

Table of Contents

Cover…… 1

SF 298…… 2

Introduction…… 4

Body…… 5

Key Research Accomplishments…… 11

Reportable Outcomes…… 11

Conclusions…… 12

References…… 14

Appendices…… 34

Award Number: DAMD17-03-1-0297

Title: Genomic and Expression Profiling of Benign and Malignant Nerve Sheath Tumors in Neurofibromatosis Patients.

INTRODUCTION

Nerve sheath tumors generally develop in the setting of neurofibromatosis (NF1), affecting 1 in 3000 individuals worldwide [1]. The most common tumor in NF1-patients is the benign 'neurofibroma'. However, about 8-13% of NF1 patients have a risk of developing malignant peripheral nerve sheath tumors (MPNSTs) [2]. MPNSTs are aggressive neoplasms that may also arise sporadically.[3, 4] Malignant transformation is a life threatening complication. The development of neurofibromas and MPNSTs involves mutations of multiple tumor suppressor genes such as NF1[5]. However, it is widely believed that mutations in tumor suppressors alone are not enough to induce peripheral nerve sheath tumor formation[6-8].

The objective of the study is to identify gene(s) that will serve as a molecular marker for patients in which the benign neurofibroma is progressing towards MPNST and to identify novel therapeutic targets for MPNSTs. We have carried out the expression profiles for over 103 nerve sheath tumors. Our initial hierarchical clustering showed high degree of variability of MPNST cases. The histological diagnosis of MPNST is difficult and often arbitrary. Our samples were obtained from a large number of collaborators and we decided to have a centralized review of histology to be performed by Dr Christopher Fletcher at Brigham & Women's Hospital, Boston. Of the 38 cases submitted as MPNST, 14 cases were reclassified. In addition all MPNST and synovial sarcoma (SS) cases underwent RT-PCR for t(X;18). After these analyses, 24 cases of classical MPNSTs and 13 cases of synovial sarcoma remained. Subsequent analysis and hierarchical clustering showed a much more interpretable result. The nerve sheath tumors revealed distinct expression signature for benign and malignant tumor types. A subset of MPNSTs clustered along with SS. Synovial sarcomas pose a major challenge in the correct diagnosis of MPNSTs. We created a large tissue microarray (TMA) with about 200 nerve sheath tumors and identified a novel diagnostic marker (TLE1) to distinguish SS from other sarcomas including MPNSTs (Terry et al., in press).

BODY

Specific aim 1: Genome wide search for genes in nerve sheath tumor

A. Gene expression profiling

A1. Collection and gene array analyses of additional cases

In the past year, to the existing gene array data on 80 nerve sheath tumor samples, we performed gene array profiling on additional 23 tumor samples. A total of 103 gene arrays were analyzed using various statistical programs. The unsupervised hierarchical clustering showed high degree of variability of MPNST cases. Initial gene array analyses of cases submitted as MPNSTs and SS yielded incomprehensible results. Diagnosis of MPNSTs poses a major challenge to pathologists; especially the histological/morphological distinction of MPNSTs from SS is a difficult task. We decided to do a centralized review of all the 54 MPNST and SS cases. Towards this, we collected the paraffin tissue blocks of all most all the MPNSTs and SS tumor samples that were included in the study.

A2. Centralized review of MPNST and SS tumor samples

A centralized review of histology for all MPNSTs and SS cases was performed by Dr Christopher Fletcher at Brigham & Women's Hospital, Boston. HE slide along with various immunostains performed on 6 unstained slides were used to review the MPNST and SS cases. We also performed RT-PCR using the SSX-SYT primers on all the MPNST and SS cases for detecting the t(X;18). The misdiagnosed tumor cases were removed from the study, and a subsequent analysis and hierarchical clustering showed a much more interpretable result.

A3. Gene expression profiling of nerve sheath tumors

In total, 87 tumor samples were used for gene array analysis, including 24 MPNSTs, 28 neurofibromas, 22 schwannomas and 13 synovial sarcomas. The microarrays used in the study contain a total of about 42000 cDNAs representing about 28 000 genes or ESTs. Only cDNA spots with a ratio of signal over background of at least 2 in either the Cy3 or Cy5 channel were included; only genes with 80% good data were included. Genes were

further selected when expression levels differed by at least four-fold in at least three arrays. Using these criteria, 5540 genes passed the filtering criteria and were used for further analysis. Unsupervised hierarchical clustering analysis [9] and significance analysis of microarrays [SAM] [10] were then performed as described previously [11]. Unsupervised analysis using average-linkage clustering, grouped the 87 tumor cases into two main groups. Most of the malignant tumors i.e MPNSTs and SS grouped in branch 'A' leaving the majority of the benign neurofibromas and schwannomas in a distinct branch 'B' (Figure 1).

Further analysis of tumor cases in branch 'A' revealed that MPNSTs and SS formed discrete groups. While the separation was not absolute most SS clustered together. A small subset of MPNSTs clustered along with SS. Interestingly the MPNSTs that clustered along with SS were all derived from male patients. The X chromosome inactivation gene '*XIST*' showed a decreased expression in those MPNST cases that clustered with SS. In contrast, XIST was highly expressed in all most all female patient samples included in this project. Synovial sarcoma is characterized with a translocation involving chromosomes X and 18 this may have some influence on clustering. However, at this point we have no clear explanation for this.

A4. Supervised analysis using significance analysis of microarrays

We subsequently analyzed the expression data by SAM, to identify and rank order the genes that differentiate various nerve sheath tumors based on their gene expression profiles. Using data from all 87 arrays, four SAM analyses were performed. First, we compared all the MPNSTs to the other tumors. Second, we analyzed genes that separated neurofibromas from the other cases. Third, we investigated the genes specifically expressed in schwannomas. Finally, the genes that distinguished SS from the other tumors were identified. The partial lists of highest ranking genes identified in these four separate SAM analyses are shown in Tables 1a, 1b, 1c and 1d respectively.

A.5. Malignant transformation in MPNSTs

A5.1. Consequences of malignant transformation in MPNSTs

The major trend in transformation from neurofibroma towards MPNST is the loss of expression of a large number of genes, rather than widespread *de novo* increase in gene expression (Figure 1). *NF1* is one of the genes for which loss of expression was noticed in most of the MPNSTs. Down regulation of large number of genes upon transformation may suggest a role for epigenetic mechanisms such as DNA hypermethylation. Further, several transcription factors including *ETS1*, *NFATC2* and *JUN* were down regulated in most MPNSTs. Examples of genes and pathways affected by transformation are shown below.

A5.2. Loss of p53 function

Inactivation of p53 serves as characteristic feature in the process of malignant transformation. As a consequence of p53 inactivation, several genes that are regulated by p53 mediated signaling are up regulated. We analyzed the expression patterns of 'inactivated p53 associated proliferation signature' genes [12] in the neurofibromas and MPNSTs. The gene expression profile analyses in nerve sheath tumors revealed that several 'p53 inactivation signature genes' such as *TOP2A, TTK, CDC2, CDC25A, HMMR, PTTG3* and *UBE2C* were up regulated in MPNSTs (Figure 2). Though most MPNSTs included in the analysis showed the signature for p53 inactivation, four MPNST tumor cases STT4734, STT4737, STT4541 and STT3920 did not show the signature for p53 loss (Figure 2). This observation suggests the presence of additional mechanisms that might lead to transformation.

A5.3. Proliferation signature

The proliferation signature includes genes responsible for the cell cycle transcriptional regulation and replication initiation complex. The proliferation signature is associated with a core set of genes such as MCM2, MCM4, MCM6, *BUB1, PLK1, CCNB2, TOP2A, FOXM1* and *MK167* [13]. Evaluating the expression profile for the core set of proliferation genes in MPNSTs and other tumors revealed that the proliferation signature was

predominantly associated with MPNSTs and SS and not with the benign tumors, neurofibroma and schwannoma (Figure 3). The proteins encoded by MCM gene family are involved in the initiation of eukaryotic genome replication and their increased expression is correlated with tumor cell proliferation [14]. MPNSTs showed increased expression for genes *MCM2*, *MCM4* and *MCM6 (figure)*. The MCM proteins are regulated by, protein kinases CDC2 and CDC7. Expression of *CDC2* and *CDC7* are highly correlated with the expression of MCM genes (Figure 3).

A5.4. Loss of cell adhesion and metastasis signature

Tumor invasion is generally associated with loss of expression of genes such as E-cadherin and over expression of the zinc-finger transcriptional repressor gene 'snail'[15-17]. In our analysis we notice the down regulation of E-cadherin (*CDH1*) in both neurofibroma and MPNSTs. Additional cell adhesion genes such as CD44, and integrins that show differential expression among nerve sheath tumors are shown in Figure 3. *TWIST1, UBE2C* and *HMMR* are highly expressed in MPNSTs, these genes are known to play a role in malignant progression [18-20] .

A6. Gene networks in MPNSTs

We have identified several gene networks (genes and its interacting partners that are functionally associated) that are differentially expressed in MPNSTs. As an example, here we discuss one of the gene networks.

Msh homeobox homologes *MSX1* and *MSX2* are highly expressed in majority of MPNSTs. These transcriptional repressors have a role in the differentiation and survival of cells. Yoshizawa et al [21] established that MSX2 co-localizes with Runx2 and Osf2 (POSTN) and suppresses its activity cooperatively, acting with another corepressor, TLE1. Our study reveals that SS expresses abundant TLE1 transcript compared to MPNSTs. Consistent to the earlier findings, in the absence of the co-repressor TLE1, expression of *POSTN* and *RUNX2* are predominantly seen in MPNSTs but not in SS. We have shown that TLE1 can be used as a diagnostic marker which can distinguish SS from MPNSTs (see below).

A7. Specific signaling pathways affected during malignant transformation in MPNSTs

To find the specific signaling pathway(s) that could be affected during malignant transformation, we carried out gene set enrichment analysis [GSEA] [22]. The program identifies genesets that are enriched in a rank ordered gene list. By comparing the expression profile of neurofibroma with MPNST, we identified several signaling pathway that could be potentially associated with the malignant transformation. Gene associated with signaling pathways such as TGFB, MET, NFKB and JAK-STAT were down regulated in MPNSTs. A list of signaling pathways and the enriched genes found that show differential expression is shown in table 2 and tables 3a-3e.

Aim 1. B: Array Comparative Genomic hybridization (aCGH)

B1. aCGH analysis of nerve sheath tumors

Using the same cDNA array platform that we used for the expression analysis, we evaluated the copy number changes of over 30 nerve sheath tumors. After the final histological diagnosis of the MPNSTs and SS, 28 arrays were selected for further analysis which includes 11 MPNSTs, 6 neurofibromas, 5 schwannomas and 6 synovial sarcomas. Tumor DNA from frozen tissue and reference DNA (normal gender-matched human leukocytes) were extracted and used in the aCHG analysis. Of the over 43,000 cDNA sequences represented on the microarrays used for this study, the chromosomal localization is known for about 21500 genes/transcripts. For CGH data the copy number for each locus was based on a moving average of the five nearest cDNA clones centered on that locus. A representative caryoscope analysis on a MPNST case which shows the gain of chromosome region 7p is shown in figure 4. A snapshot of 7p21.1 genomic locus amplification in majority of MPNSTs, which harbors *TWIST1,* is shown in Figure 5.

<u>Specific Aim 2: Validation of candidate genes on large numbers of cases using immunohistochemistry and *in situ* hybridization on TMA.</u>

A1. Construction of nerve sheath tumor tissue array

In the previous annual report we described the construction of a tissue microarray (TA-138) containing 68 MPNSTs, 42 neurofibromas, 22 schwannomas and 15 synovial

sarcomas. To our knowledge, this remains the largest TMA of nerve sheath tumors. In the past year we have made in situ hybridization probes for several differentially expressed genes in nerve sheath tumors such as *FGFR1*, *FGFR2*, *FGFR3*, and *CD44*. Analysis of these and other genes on TA-138 is ongoing. Using immunohistochemistry (IHC) we have analyzed the expression of EGFR in nerve sheath tumors. Consistent with the gene array findings our TMA analyses revealed that a subset of MPNSTs show strong expression of EGFR. Representative MPNST staining for EGFR is shown in Figure 6. Further we have titred many antibodies (ZIC1, TTK, L1CAM, ERBB3, TLE3, PLA2R1, TNSF10, PTTG1, TBX3, FAT, TFP1, and PLA2G2A) to allow staining on TA-138
We have managed to collect the paraffin tissue blocks for all most all the MPNST and SS cases that were used in our gene array study. From these paraffin blocks a tissue microarray will be constructed. Staining this TMA with potential biomarkers selected from our gene array studies will serve as a direct confirmation for our gene array data.

A2. TLE1 as a novel diagnostic marker for synovial sarcoma

Synovial sarcoma is a soft tissue malignancy defined by the SYT-SSX fusion oncogene. Gene expression profiling studies performed by us and other groups have consistently identified TLE1 as an excellent discriminator of synovial sarcoma from other sarcomas, including histologically similar tumors such as MPNSTs. TLE proteins (human homologues of groucho) are transcriptional corepressors that have an established role in repressing differentiation. We examined the expression of TLE proteins in SS and in a broad range of mesenchymal tumors using tissue microarrays to assess the value of anti-TLE antibodies in the immunohistochemical confirmation of synovial sarcoma. We have demonstrated that TLE expression is a consistent feature of SS. TLE shows intense and/or diffuse nuclear staining in 91/94 molecularly-confirmed synovial sarcomas. In contrast, TLE staining is detected much less frequently and at lower levels, if at all, in 40 other mesenchymal tumors. (Please see the attached manuscript in press for details)

KEY RESEARCH ACCOMPLISHMENTS

1. Gene expression profiling on a large number (87 cases) of nerve sheath tumors and the related lesion synovial sarcoma

- Bioinformatical and statistical analyses to characterize molecular events that are potentially associated with malignant transformation.
- Identification of genes and gene networks that are potentially associated with malignant transformation.

2. Array comparative genome hybridization.

3. Development of diagnostic marker for synovial sarcoma

REPORTABLE OUTCOMES:

Abstract

Subramanian S, West RB, Nielsen TO, Rubin BP, Downs-Kelly E, Goldblum JR, Zhu S, Montgomery K, Hogendoorn PCW, Corless CL, Oliveira AM, Fletcher CDM and van de Rijn M. Genome-wide transcriptome analysis of nerve sheath tumors (2006) 97th Annual meeting of American Association of Cancer Research AACR Washington DC. USA (Poster)

Publication

Terry J, Saito T, Subramanian S, Cindy R, Antonescu CR, Goldblum JR, Downs-Kelly E, Corless CL, Rubin BP, van de Rijn M, Ladanyi M, and Nielsen TO.TLE1 as a diagnostic immunohistochemical marker for synovial sarcoma emerging form gene expression profiling studies. 2006 *Am J Surg Path* (in press)

CONCLUSIONS

In the past year we have performed gene microarray experiments on a significant number of additional cases of MPNSTs, neurofibromas, schwannomas, and synovial sarcomas for a total of 103 specimens. Correct diagnosis of MPNSTs poses a major challenge to pathologists; especially the histological/morphological distinction of MPNSTs from SS is a difficult task. In order to use MPNST and SS tumor samples with correct diagnosis in our gene expression studies, we have spent considerable amount of time in collecting and organizing the paraffin tissue blocks for all the 54 MPNST and SS cases that were analyzed by gene arrays.

Dr Christopher Fletcher kindly agreed to review all the MPNST and SS cases. It can be appreciated that the gene expression data after the centralized review by Dr Fletcher is much cleaner and appealing as compared to the last year's clusters that we submitted in our 2005 annual reports. As a further , molecular confirmation of the diagnosis, we determined the presence or absence of the SSX-SYT fusion transcript for all most all cases of MPNSTs and SS by RT-PCR. For those cases where no RNA was available, fluorescence in situ hybridization (FISH) was performed on paraffin sections to detect the X:18 translocation. We have carried out considerable amount of data analyses, literature searches and pathway analysis to characterize the molecular events that are associated with malignant transformation.

In the past year we also performed array comparative genomic hybridization experiments for 28 cases nerve sheath tumor cases including 6 SS. We identified loss and gain of genomic regions in nerve sheath tumor types. Many of the chromosomal aberrations that we noticed have previously been reported in the literature. We noticed that in a subset of MPNSTs, amplification of the locus 7p21 occurs. This locus harbors *TWIST1*, the gene responsible for tumor metastasis. In addition to testing several antibodies on TMA for their potential to be a diagnostic marker, we have constructed several ISH probes that are currently being studied.

In an extraordinary collaboration among the three collaborating institutions on this grant (Stanford University Medical Center, University of British Columbia, University of Washington), we have been able to generate and analyze a signification amount of gene array and aCHG data. We have presented a portion of our findings in the annual meeting

of American association for cancer research and were able to submit a manuscript that describes a novel diagnostic marker for SS. Currently we are writing up the manuscript on the gene array analysis of nerve sheath tumors that will be soon be submitted for publication.

References

1. Huson SM, Compston DA, Clark P, Harper PS: A genetic study of von Recklinghausen neurofibromatosis in south east Wales. I. Prevalence, fitness, mutation rate, and effect of parental transmission on severity, J Med Genet 1989, 26:704-711
2. Evans DG, Baser ME, McGaughran J, Sharif S, Howard E, Moran A: Malignant peripheral nerve sheath tumours in neurofibromatosis 1, J Med Genet 2002, 39:311-314
3. Cichowski K, Jacks T: NF1 tumor suppressor gene function: narrowing the GAP, Cell 2001, 104:593-604
4. Riccardi VM: Von Recklinghausen neurofibromatosis, N Engl J Med 1981, 305:1617-1627
5. Dasgupta B, Dugan LL, Gutmann DH: The neurofibromatosis 1 gene product neurofibromin regulates pituitary adenylate cyclase-activating polypeptide-mediated signaling in astrocytes, J Neurosci 2003, 23:8949-8954
6. Kourea HP, Orlow I, Scheithauer BW, Cordon-Cardo C, Woodruff JM: Deletions of the INK4A gene occur in malignant peripheral nerve sheath tumors but not in neurofibromas, Am J Pathol 1999, 155:1855-1860
7. Legius E, Dierick H, Wu R, Hall BK, Marynen P, Cassiman JJ, Glover TW: TP53 mutations are frequent in malignant NF1 tumors, Genes Chromosomes Cancer 1994, 10:250-255
8. Menon AG, Anderson KM, Riccardi VM, Chung RY, Whaley JM, Yandell DW, Farmer GE, Freiman RN, Lee JK, Li FP, et al.: Chromosome 17p deletions and p53 gene mutations associated with the formation of malignant neurofibrosarcomas in von Recklinghausen neurofibromatosis, Proc Natl Acad Sci U S A 1990, 87:5435-5439
9. Eisen MB, Spellman PT, Brown PO, Botstein D: Cluster analysis and display of genome-wide expression patterns, Proc Natl Acad Sci U S A 1998, 95:14863-14868
10. Tusher VG, Tibshirani R, Chu G: Significance analysis of microarrays applied to the ionizing radiation response, Proc Natl Acad Sci U S A 2001, 98:5116-5121
11. Nielsen TO, West RB, Linn SC, Alter O, Knowling MA, O'Connell JX, Zhu S, Fero M, Sherlock G, Pollack JR, Brown PO, Botstein D, van de Rijn M: Molecular characterisation of soft tissue tumours: a gene expression study, Lancet 2002, 359:1301-1307
12. Milyavsky M, Tabach Y, Shats I, Erez N, Cohen Y, Tang X, Kalis M, Kogan I, Buganim Y, Goldfinger N, Ginsberg D, Harris CC, Domany E, Rotter V: Transcriptional programs following genetic alterations in p53, INK4A, and H-Ras genes along defined stages of malignant transformation, Cancer Res 2005, 65:4530-4543
13. Whitfield ML, George LK, Grant GD, Perou CM: Common markers of proliferation, Nat Rev Cancer 2006, 6:99-106
14. Perou CM, Jeffrey SS, van de Rijn M, Rees CA, Eisen MB, Ross DT, Pergamenschikov A, Williams CF, Zhu SX, Lee JC, Lashkari D, Shalon D, Brown PO, Botstein D: Distinctive gene expression patterns in human mammary epithelial cells and breast cancers, Proc Natl Acad Sci U S A 1999, 96:9212-9217
15. Batlle E, Sancho E, Franci C, Dominguez D, Monfar M, Baulida J, Garcia De Herreros A: The transcription factor snail is a repressor of E-cadherin gene expression in epithelial tumour cells, Nat Cell Biol 2000, 2:84-89

16. Behrens J, Mareel MM, Van Roy FM, Birchmeier W: Dissecting tumor cell invasion: epithelial cells acquire invasive properties after the loss of uvomorulin-mediated cell-cell adhesion, J Cell Biol 1989, 108:2435-2447
17. Cano A, Perez-Moreno MA, Rodrigo I, Locascio A, Blanco MJ, del Barrio MG, Portillo F, Nieto MA: The transcription factor snail controls epithelial-mesenchymal transitions by repressing E-cadherin expression, Nat Cell Biol 2000, 2:76-83
18. Okamoto Y, Ozaki T, Miyazaki K, Aoyama M, Miyazaki M, Nakagawara A: UbcH10 is the cancer-related E2 ubiquitin-conjugating enzyme, Cancer Res 2003, 63:4167-4173
19. Rein DT, Roehrig K, Schondorf T, Lazar A, Fleisch M, Niederacher D, Bender HG, Dall P: Expression of the hyaluronan receptor RHAMM in endometrial carcinomas suggests a role in tumour progression and metastasis, J Cancer Res Clin Oncol 2003, 129:161-164
20. Yang J, Mani SA, Donaher JL, Ramaswamy S, Itzykson RA, Come C, Savagner P, Gitelman I, Richardson A, Weinberg RA: Twist, a master regulator of morphogenesis, plays an essential role in tumor metastasis, Cell 2004, 117:927-939
21. Yoshizawa T, Takizawa F, Iizawa F, Ishibashi O, Kawashima H, Matsuda A, Endo N, Kawashima H: Homeobox protein MSX2 acts as a molecular defense mechanism for preventing ossification in ligament fibroblasts, Mol Cell Biol 2004, 24:3460-3472
22. Subramanian A, Tamayo P, Mootha VK, Mukherjee S, Ebert BL, Gillette MA, Paulovich A, Pomeroy SL, Golub TR, Lander ES, Mesirov JP: Gene set enrichment analysis: a knowledge-based approach for interpreting genome-wide expression profiles, Proc Natl Acad Sci U S A 2005, 102:15545-15550

LEGENDS FOR FIGURES

Figure 1
Unsupervised hierarchical cluster analysis of gene expression profiles of 87 nerve sheath tumors and SS along with the heat map of the 5540 genes used for generating hierarchical clustering. Each row represents the relative levels of expression for a single gene. Each column shows the expression levels for a single sample. The red or green color indicates high or low expression, respectively.

Figure 2
Expression profiles of genes that are associated with the inactivation of p53.

Figure 3
Overview of expression pattern of selected genes involved in cell cycle regulation, cell adhesion, metastasis and gene networks etc.

Figure 4
A representative caryoscope generated for MPNST by determining loss or amplification in chromosomes (CLAC) using CGH-miner program.

Figure 5
A screenshot showing the copy number increase in p-arm of chromosome 7 and the associated genes in that locus.

Figure 6
Representative cores showing strong positive and negative immunohistochemistry staining of EGFR in MPNSTs. a) Strong expression of EGFR in MPNST; b) absence of EGFR expression in MPNST.

LEGEND FOR TABLES

Table 1a
A partial list of genes with highest differential expression in MPNSTs according to SAM analysis.

Table 1b
A partial list of genes with highest differential expression in neurofibromas according to SAM analysis.

Table 1c
A partial list of genes with highest differential expression in schwannomas according to SAM analysis.

Table 1d
A partial list of genes with highest differential expression in synovial sarcomas according to SAM analysis.

Table 2
Signaling pathways identified by gene set enrichment analysis method that are affected during the malignant transformation.

Table 3a-e
Signaling pathway and the associated genes that show differential expression in our gene array analyses.

Figure 1

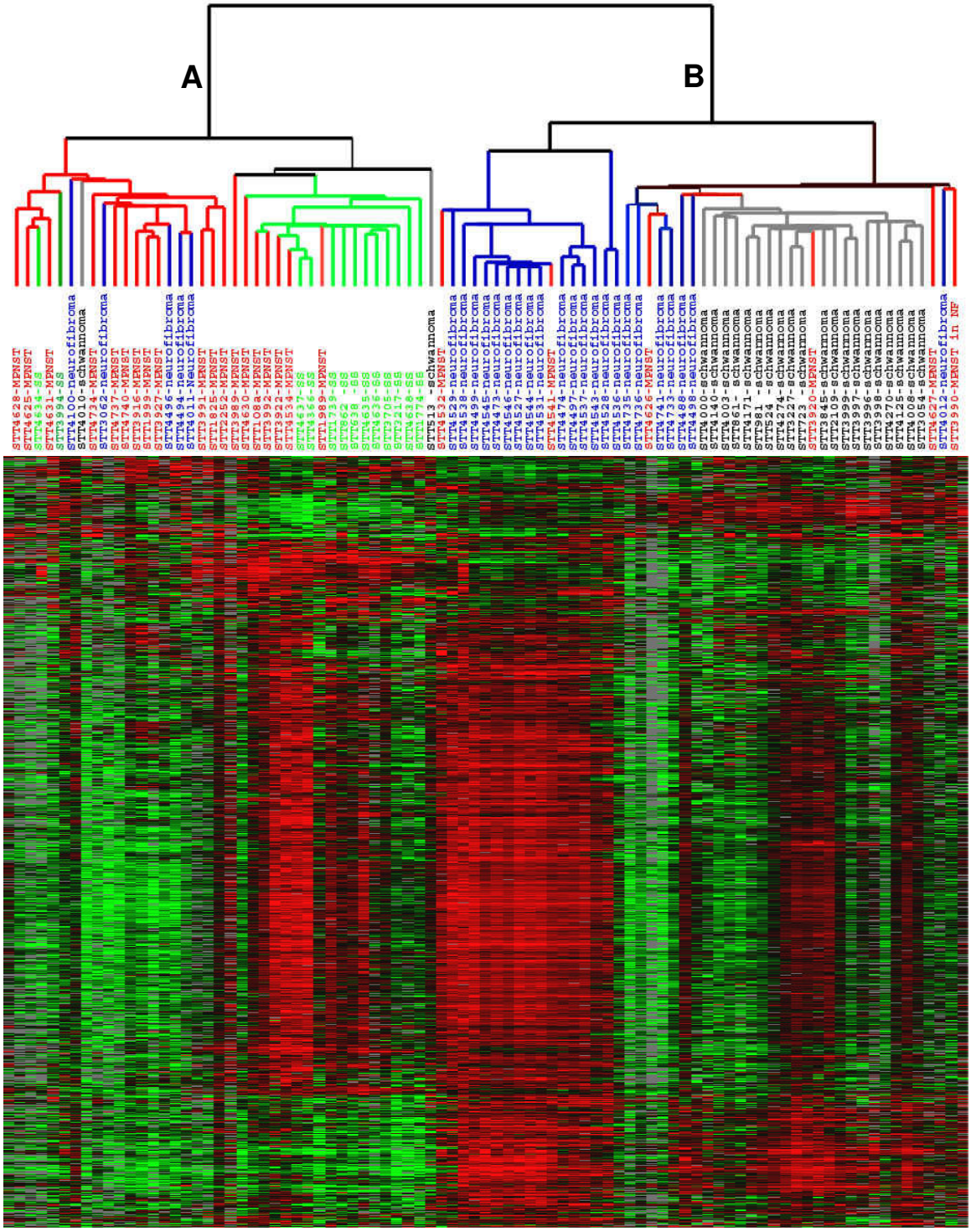
A
B
STT4628-MPNST
STT4625-MPNST
STT4634-SS
STT4631-MPNST
STT4634-SS
STT4100-neurofibroma
STT4010-schwannoma
STT3062-neurofibroma
STT4734-MPNST
STT4737-MPNST
STT4740-MPNST
STT3916-MPNST
STT1999-MPNST
STT3927-MPNST
STT4496-neurofibroma
STT4494-neurofibroma
STT4401-neurofibroma
STT3991-MPNST
STT1925-MPNST
STT3989-MPNST
STT4630-MPNST
STT1108a-MPNST
STT3992-MPNST
STT3922-MPNST
STT4534-MPNST
STT4637-SS
STT4366-SS
STT1989-MPNST
STT1739-SS
STT852 -SS
STT638 -SS
STT4653-SS
STT3705-SS
STT3317-SS
STT4638-SS
STT174-SS
STT513 -schwannoma
STT4532-MPNST
STT4529-neurofibroma
STT4538-neurofibroma
STT4499-neurofibroma
STT4545-neurofibroma
STT4473-neurofibroma
STT4546-neurofibroma
STT4527-neurofibroma
STT4544-neurofibroma
STT4641-MPNST
STT4474-neurofibroma
STT4497-neurofibroma
STT4537-neurofibroma
STT4543-neurofibroma
STT4528-neurofibroma
STT4536-neurofibroma
STT4735-neurofibroma
STT4736-neurofibroma
STT4626-MPNST
STT4741-neurofibroma
STT4733-neurofibroma
STT4498-neurofibroma
STT4000-schwannoma
STT4003-schwannoma
STT4140-schwannoma
STT861 -schwannoma
STT4171-schwannoma
STT981 -schwannoma
STT524 -schwannoma
STT4274-schwannoma
STT3227-schwannoma
STT723 -schwannoma
STT3920-MPNST
STT3845-schwannoma
STT2399-schwannoma
STT3997-schwannoma
STT3996-schwannoma
STT3998-schwannoma
STT4270-schwannoma
STT4125-schwannoma
STT4008-schwannoma
STT3054-schwannoma
STT4627-MPNST
STT4012-neurofibroma
STT3990-MPNST in NF

Figure 2

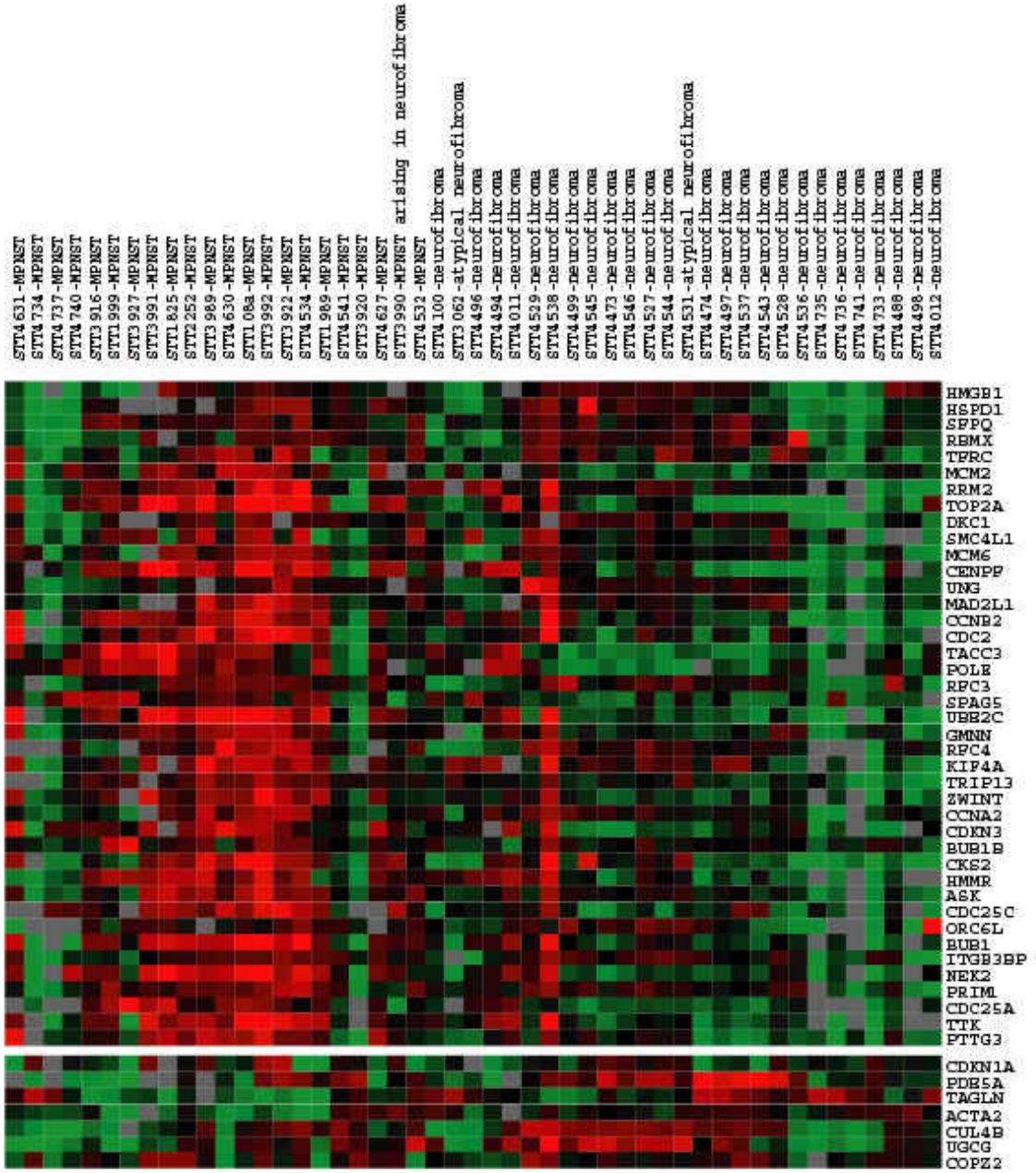
STT4631-MPNST
STT4734-MPNST
STT4737-MPNST
STT4740-MPNST
STT3916-MPNST
STT1999-MPNST
STT3927-MPNST
STT3991-MPNST
STT1825-MPNST
STT2252-MPNST
STT3989-MPNST
STT4630-MPNST
STT1108a-MPNST
STT3992-MPNST
STT3912-MPNST
STT4534-MPNST
STT1989-MPNST
STT4541-MPNST
STT3920-MPNST
STT4627-MPNST
STT3990-MPNST arising in neurofibroma
STT4532-MPNST
STT4100-neurofibroma
STT3062-atypical neurofibroma
STT4496-neurofibroma
STT4494-neurofibroma
STT4011-neurofibroma
STT4529-neurofibroma
STT4538-neurofibroma
STT4499-neurofibroma
STT4545-neurofibroma
STT4473-neurofibroma
STT4546-neurofibroma
STT4527-neurofibroma
STT4544-neurofibroma
STT4531-atypical neurofibroma
STT4474-neurofibroma
STT4497-neurofibroma
STT4537-neurofibroma
STT4543-neurofibroma
STT4528-neurofibroma
STT4536-neurofibroma
STT4735-neurofibroma
STT4736-neurofibroma
STT4741-neurofibroma
STT4733-neurofibroma
STT4488-neurofibroma
STT4498-neurofibroma
STT4012-neurofibroma
HMGB1
HSPD1
SFPQ
RBMX
TFRC
MCM2
RRM2
TOP2A
DKC1
SMC4L1
MCM6
CENPF
UNG
MAD2L1
CCNB2
CDC2
TACC3
POLE
RFC3
SPAG5
UBE2C
GMNN
RFC4
KIF4A
TRIP13
ZWINT
CCNA2
CDKN3
BUB1B
CKS2
HMMR
ASK
CDC25C
ORC6L
BUB1
ITGB3BP
NEK2
PRIM1
CDC25A
TTK
PTTG3
CDKN1A
PDE5A
TAGLN
ACTA2
CUL4B
UGCG
COPZ2

Figure 3

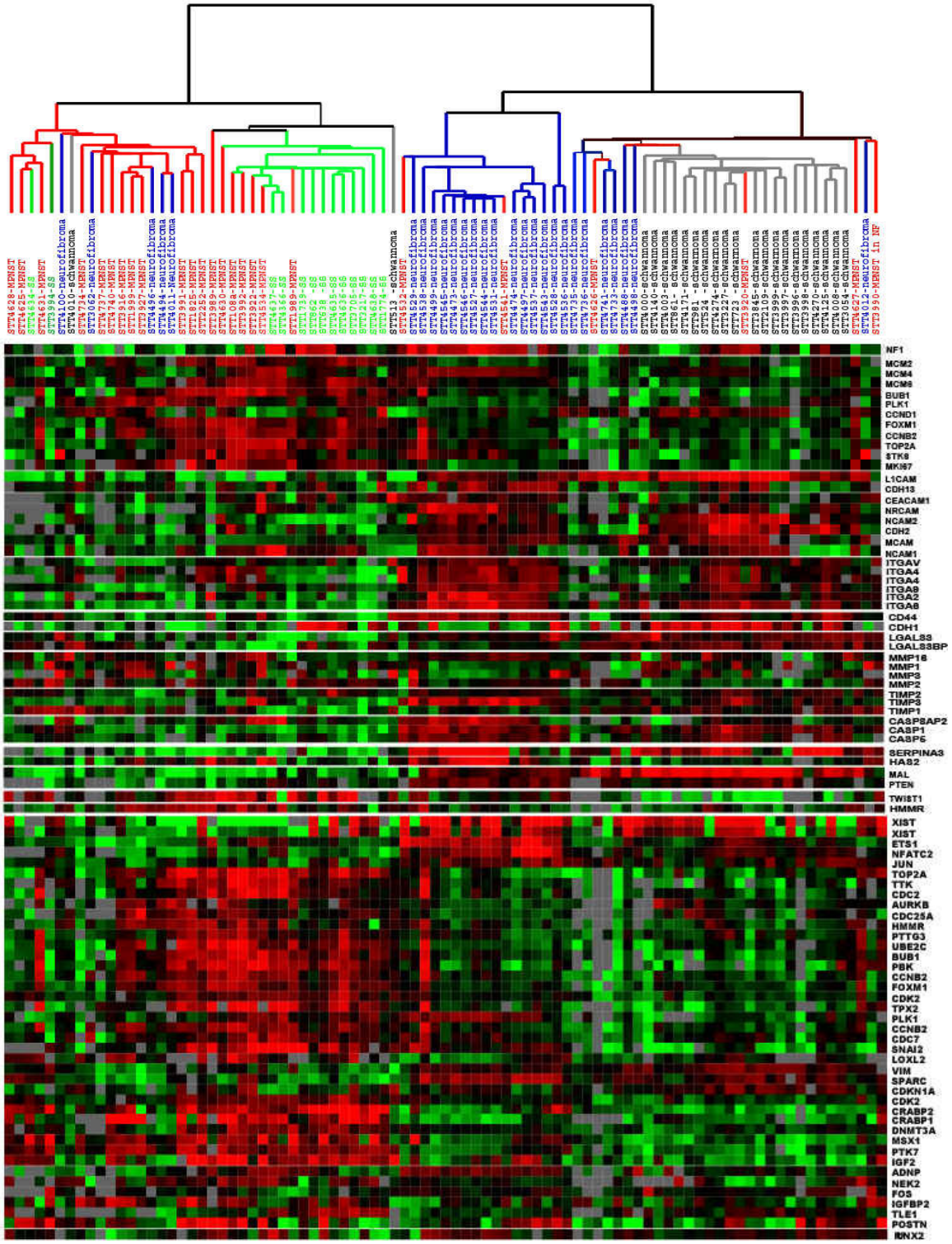
NF1
MCM2
MCM4
MCM6
BUB1
PLK1
CCND1
FOXM1
CCNB2
TOP2A
STK6
MKI67
L1CAM
CDH13
CEACAM1
NRCAM
NCAM2
CDH2
MCAM
NCAM1
ITGAV
ITGA4
ITGA4
ITGA9
ITGA2
ITGA8
CD44
CDH1
LGALS3
LGALS3BP
MMP16
MMP1
MMP3
MMP2
TIMP2
TIMP3
TIMP1
CASP8AP2
CASP1
CASP5
SERPINA3
HAS2
MAL
PTEN
TWIST1
HMMR
XIST
XIST
ETS1
NFATC2
JUN
TOP2A
TTK
CDC2
AURKB
CDC25A
HMMR
PTTG3
UBE2C
BUB1
PBK
CCNB2
FOXM1
CDK2
TPX2
PLK1
CCNB2
CDC7
SNAI2
LOXL2
VIM
SPARC
CDKN1A
CDK2
CRABP2
CRABP1
DNMT3A
MSX1
PTK7
IGF2
ADNP
NEK2
FOS
IGFBP2
TLE1
POSTN
RNX2

Figure 4

CLAC Plot for Sample: shgt157 aCGH:STT1999–MPNST||shgt157 ; (FDR=1.124)

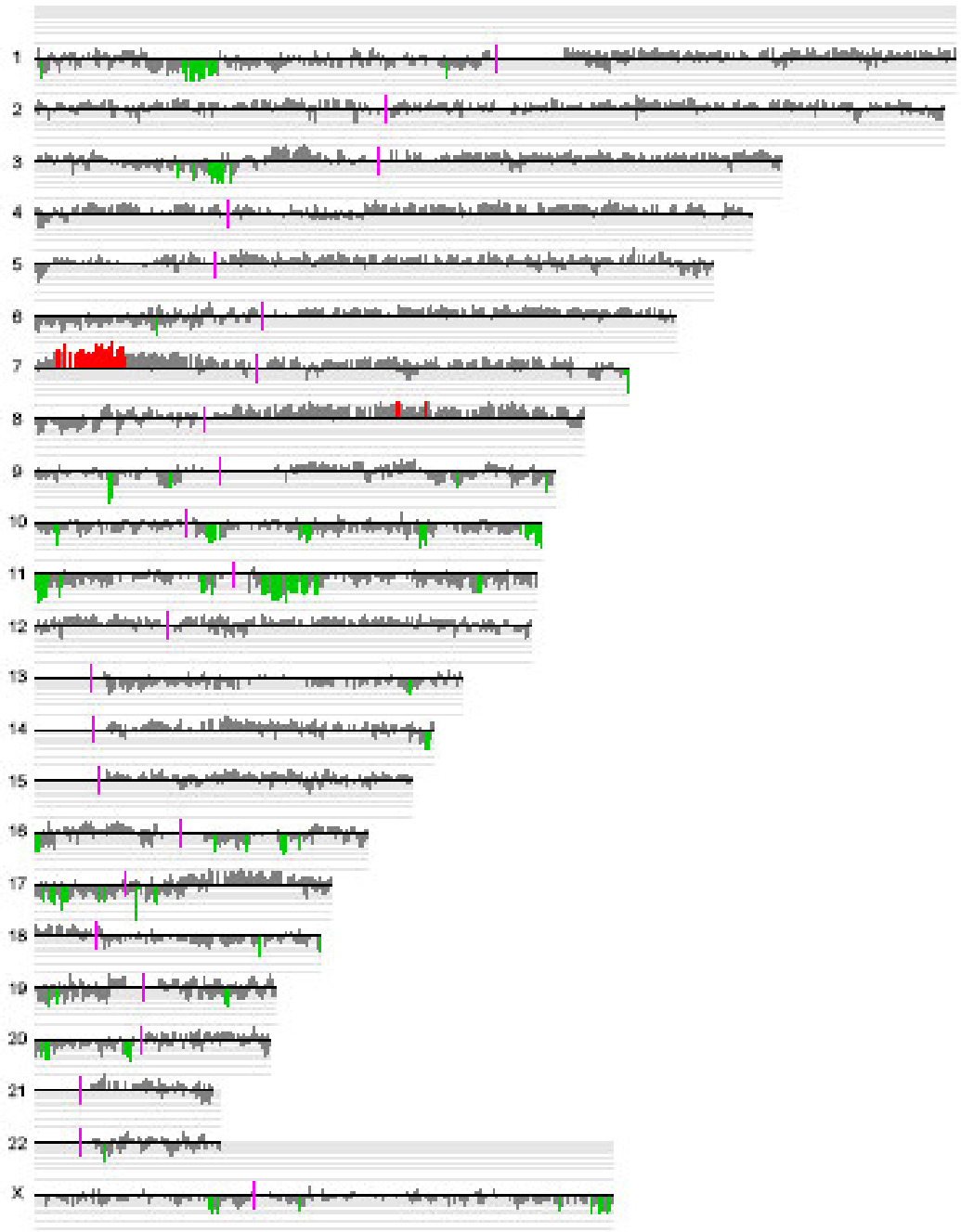

Figure 5

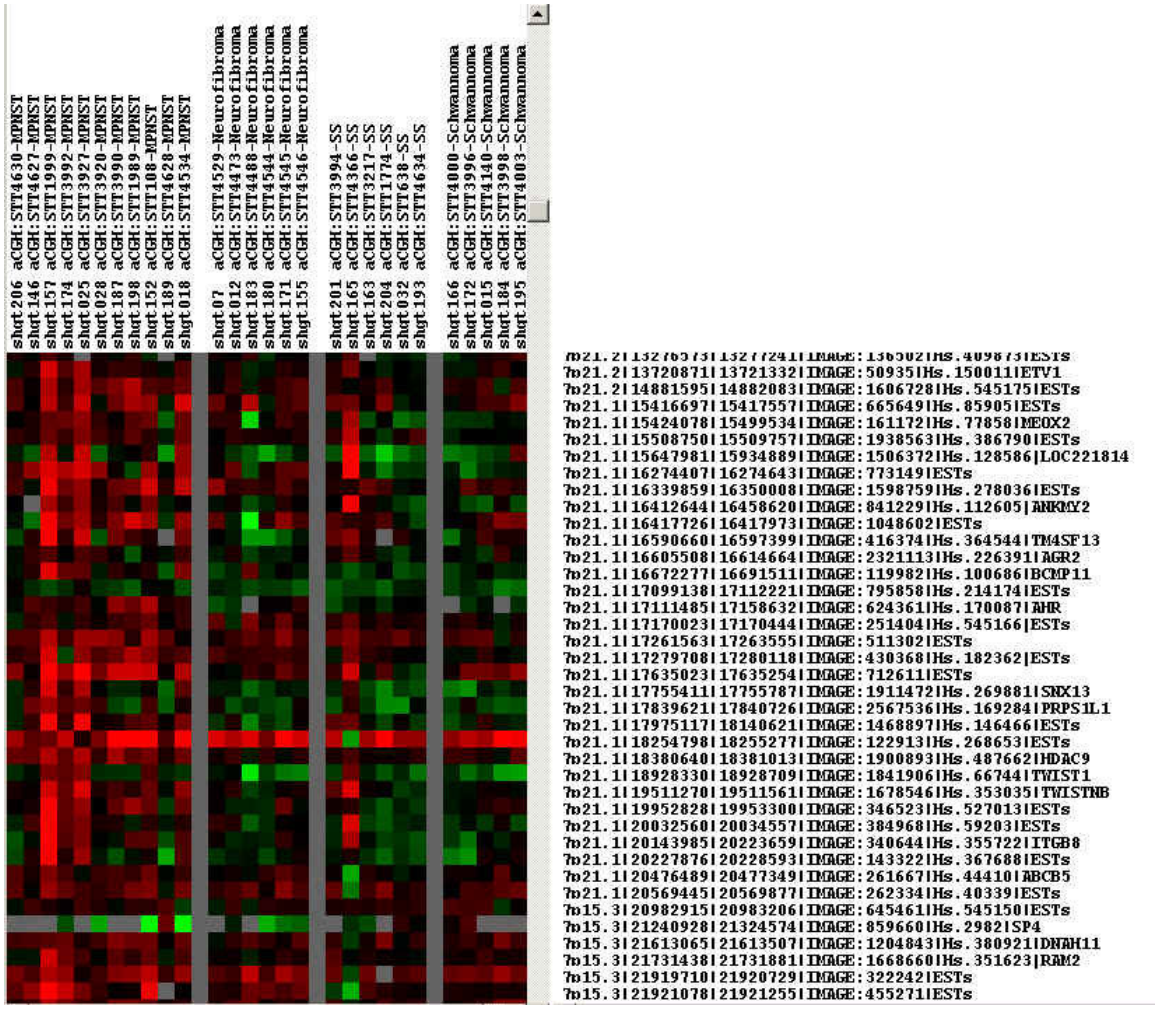
shgt206 aCGH:STT4630-MPNST
shgt146 aCGH:STT4627-MPNST
shgt157 aCGH:STT1999-MPNST
shgt174 aCGH:STT3992-MPNST
shgt025 aCGH:STT3927-MPNST
shgt028 aCGH:STT3920-MPNST
shgt187 aCGH:STT3990-MPNST
shgt198 aCGH:STT1989-MPNST
shgt152 aCGH:STT108-MPNST
shgt189 aCGH:STT4628-MPNST
shgt018 aCGH:STT4534-MPNST
shgt07 aCGH:STT4529-Neurofibroma
shgt012 aCGH:STT4473-Neurofibroma
shgt183 aCGH:STT4488-Neurofibroma
shgt180 aCGH:STT4544-Neurofibroma
shgt171 aCGH:STT4545-Neurofibroma
shgt155 aCGH:STT4546-Neurofibroma
shgt201 aCGH:STT3994-SS
shgt165 aCGH:STT4366-SS
shgt163 aCGH:STT3217-SS
shgt204 aCGH:STT1774-SS
shgt032 aCGH:STT638-SS
shgt193 aCGH:STT4634-SS
shgt166 aCGH:STT4000-Schwannoma
shgt172 aCGH:STT3996-Schwannoma
shgt015 aCGH:STT4140-Schwannoma
shgt184 aCGH:STT3998-Schwannoma
shgt195 aCGH:STT4003-Schwannoma
7b21.2|13276573|13277241|IMAGE:136502|Hs.409873|ESTs
7b21.2|13720871|13721332|IMAGE:50935|Hs.150011|ETV1
7b21.2|14881595|14882083|IMAGE:1606728|Hs.545175|ESTs
7b21.1|15416697|15417557|IMAGE:665649|Hs.85905|ESTs
7b21.1|15424078|15499534|IMAGE:161172|Hs.77858|MEOX2
7b21.1|15508750|15509757|IMAGE:1938563|Hs.386790|ESTs
7b21.1|15647981|15934889|IMAGE:1506372|Hs.128586|LOC221814
7b21.1|16274407|16274643|IMAGE:773149|ESTs
7b21.1|16339859|16350008|IMAGE:1598759|Hs.278036|ESTs
7b21.1|16412644|16458620|IMAGE:841229|Hs.112605|ANKMY2
7b21.1|16417726|16417973|IMAGE:1048602|ESTs
7b21.1|16590660|16597399|IMAGE:416374|Hs.364544|TM4SF13
7b21.1|16605508|16614664|IMAGE:2321113|Hs.226391|AGR2
7b21.1|16672277|16691511|IMAGE:119982|Hs.100686|BCMP11
7b21.1|17099138|17112221|IMAGE:795858|Hs.214174|ESTs
7b21.1|17111485|17158632|IMAGE:624361|Hs.170087|AHR
7b21.1|17170023|17170444|IMAGE:251404|Hs.545166|ESTs
7b21.1|17261563|17263555|IMAGE:511302|ESTs
7b21.1|17279708|17280118|IMAGE:430368|Hs.182362|ESTs
7b21.1|17635023|17635254|IMAGE:712611|ESTs
7b21.1|17755411|17755787|IMAGE:1911472|Hs.269881|SNX13
7b21.1|17839621|17840726|IMAGE:2567536|Hs.169284|PRPS1L1
7b21.1|17975117|18140621|IMAGE:1468897|Hs.146466|ESTs
7b21.1|18254798|18255277|IMAGE:122913|Hs.268653|ESTs
7b21.1|18380640|18381013|IMAGE:1900893|Hs.487662|HDAC9
7b21.1|18928330|18928709|IMAGE:1841906|Hs.66744|TWIST1
7b21.1|19511270|19511561|IMAGE:1678546|Hs.353035|TWISTNB
7b21.1|19952828|19953300|IMAGE:346523|Hs.527013|ESTs
7b21.1|20032560|20034557|IMAGE:384968|Hs.59203|ESTs
7b21.1|20143985|20223659|IMAGE:340644|Hs.355722|ITGB8
7b21.1|20227876|20228593|IMAGE:143322|Hs.367688|ESTs
7b21.1|20476489|20477349|IMAGE:261667|Hs.44410|ABCB5
7b21.1|20569445|20569877|IMAGE:262334|Hs.40339|ESTs
7b15.3|20982915|20983206|IMAGE:645461|Hs.545150|ESTs
7b15.3|21240928|21324574|IMAGE:859660|Hs.2982|SP4
7b15.3|21613065|21613507|IMAGE:1204843|Hs.380921|DNAH11
7b15.3|21731438|21731881|IMAGE:1668660|Hs.351623|RAM2
7b15.3|21919710|21920729|IMAGE:322242|ESTs
7b15.3|21921078|21921255|IMAGE:455271|ESTs

Figure 6

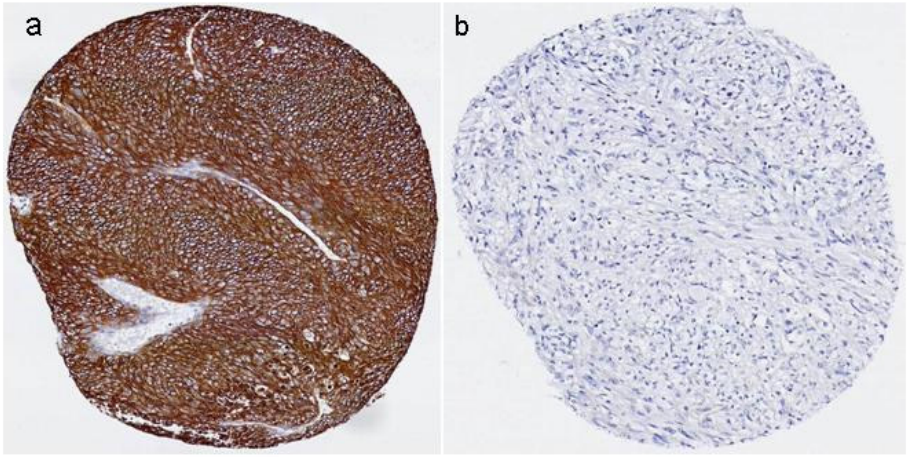

Table 1a

Gene ID	Gene Nar	Score(d)	Numerator(r	Denominator(s+s0)	Fold Change	q-value(%)
|| || Transcribed locus || Hs.563006 || 109176	1	2.834164779	1.96213277	0.692314288	1.74933517	0
|| MEST || Mesoderm specific transcript homolog (mou	1	2.834070954	1.48733136	0.524803855	2.656708	0
|| SEMA3A || Sema domain, immunoglobulin domain (	1	2.797788068	1.65449748	0.591359117	2.01760143	0
|| || || || 311247	1	2.795096772	1.58081866	0.565568491	3.65793119	0
|| DLK1 || Delta-like 1 homolog (Drosophila) || Hs.5337	1	2.740168449	2.4024471	0.876751611	3.99590244	0
|| GATA3 || GATA binding protein 3 || Hs.524134 || 101	1	2.735315709	1.42643888	0.521489666	1.65427509	0
|| EIF2B3 || **Eukaryotic translation initiation factor 2B	1	2.72409874	1.95833734	0.71889367	1.79573195	0
|| CRABP1 || Cellular retinoic acid binding protein 1 || H	1	2.708004868	1.79335949	0.662243819	2.62360169	0
|| C7orf30 || **Chromosome 7 open reading frame 30 ||	1	2.695964132	1.21754194	0.451616519	2.73870014	0
|| CRABP1 || Cellular retinoic acid binding protein 1 || H	1	2.678193258	1.95121059	0.728554815	2.62166022	0
|| CPA3 || Carboxypeptidase A3 (mast cell) || Hs.646 |	1	2.642648787	1.63811502	0.619876173	2.1206464	0
|| PTK7 || **PTK7 protein tyrosine kinase 7 || Hs.90572	1	2.624436801	1.3881871	0.528946666	2.25544653	0
|| MSX1 || Msh homeo box homolog 1 (Drosophila) || H	1	2.595013901	1.5428	0.594524754	1.68495479	0
|| SEMA3A || Sema domain, immunoglobulin domain (	1	2.579686609	1.48643065	0.5762059	2.1681315	0.155871
|| PCOLCE || Procollagen C-endopeptidase enhancer |	1	2.553936477	1.3243862	0.518566618	2.33491019	0.155871
|| CDC25C || Cell division cycle 25C || Hs.656 || 10780	1	2.54241504	1.27106807	0.49994515	2.42517082	0.155871
|| TWIST1 || Twist homolog 1 (acrocephalosyndactyly	1	2.477659329	1.58447464	0.639504642	1.99273416	0.155871
|| NEK2 || NIMA (never in mitosis gene a)-related kinas	1	2.453772274	1.38526487	0.564545003	2.78719512	0.263675
|| PYCR1 || Pyrroline-5-carboxylate reductase 1 || Hs.4	1	2.450170238	1.26515914	0.516355607	2.68954056	0.263675
|| MAPK7 || Mitogen-activated protein kinase 7 || Hs.15	1	2.443673444	1.07468978	0.439784533	2.06086749	0.263675
|| LOXL2 || Lysyl oxidase-like 2 || Hs.116479 || 114413	1	2.42454404	1.08726804	0.448442271	2.3649708	0.263675
|| SOX4 || SRY (sex determining region Y)-box 4 || Hs.	1	2.422517913	1.09339355	0.451345909	2.2274716	0.263675
|| PCOLCE || Procollagen C-endopeptidase enhancer |	1	2.411383867	1.22883817	0.509598737	1.88517645	0.263675
|| KIAA0101 || KIAA0101 || Hs.81892 || 115900	1	2.399753154	1.3918055	0.57997861	2.52531365	0.263675
|| THBS4 || Thrombospondin 4 || Hs.211426 || 119951	1	2.367300866	1.34859946	0.569678101	3.0266392	0.331436
|| POSTN || Periostin, osteoblast specific factor || Hs.1	1	2.344295225	1.61655197	0.689568427	2.4372523	0.380451
|| DLG7 || Discs, large homolog 7 (Drosophila) || Hs.77	1	2.300111514	1.38762938	0.60328787	2.7864496	0.541556
|| UBE2C || Ubiquitin-conjugating enzyme E2C || Hs.93	1	2.294886553	1.28415726	0.559573307	3.29303302	0.541556
|| MRC2 || Mannose receptor, C type 2 || Hs.7835 || 11	1	2.246300766	1.03514487	0.460822028	1.97127092	0.62084
|| ADNP || Activity-dependent neuroprotector || Hs.293	1	2.243387009	1.03119293	0.459658957	1.84716054	0.62084
|| LOC388152 || Hypothetical protein FLJ90297 || Hs.4	1	2.23629343	0.9725651	0.434900486	1.90720712	0.62084
|| TPX2 || TPX2, microtubule-associated, homolog (Xer	1	2.220806951	1.40647577	0.633317439	2.49893165	0.62084
|| CTHRC1 || Collagen triple helix repeat containing 1 ||	1	2.201981441	1.21440124	0.551503847	2.37237273	0.62084
|| DLK1 || Delta-like 1 homolog (Drosophila) || Hs.5337	1	2.185263084	1.88921587	0.864525597	3.95124394	0.771826
|| ELN || Elastin (supravalvular aortic stenosis, William	1	2.177267457	1.183165	0.543417389	2.25469337	0.771826
|| FLJ12505 || Hypothetical protein FLJ12505 || Hs.968	1	2.171623144	1.43649849	0.661486083	1.66080485	0.771826
|| CDKN3 || Cyclin-dependent kinase inhibitor 3 (CDK2	1	2.162243036	1.01874214	0.471150617	2.40635839	0.771826
|| IGFBP2 || Insulin-like growth factor binding protein 2	1	2.16132683	1.13202857	0.523765566	2.49249236	0.771826

Table 1b

Gene ID	Gene Nai	Score(d)	Numerator(r	Denominator(s+s0)	Fold Change	q-value(%)
|| TFPI || Tissue factor pathway inhibitor (lipop	1	4.613441221	2.35827778	0.511175425	3.59386882	0
|| TFPI || Tissue factor pathway inhibitor (lipop	1	4.229299539	2.19805787	0.519721493	3.00064105	0
|| PALMD || Palmdelphin || Hs.483993 || 2252	1	4.178120688	2.2160006	0.530382141	5.1625263	0
|| ADH1B || Alcohol dehydrogenase IB (class	1	4.134088114	2.59839167	0.628528371	3.6483497	0
|| PALMD || Palmdelphin || Hs.483993 || 3148	1	3.940705439	1.97443651	0.501036309	4.58785848	0
|| PALMD || Palmdelphin || Hs.483993 || 1105	1	3.763405196	2.18851058	0.581524037	5.65771928	0
|| ELOVL2 || Elongation of very long chain fatt	1	3.734113866	2.18187784	0.584309403	5.3985426	0
|| DSCR1L1 || Down syndrome critical region	1	3.717612014	1.8225	0.490234052	3.39972502	0
|| ABCG2 || ATP-binding cassette, sub-family	1	3.687550758	1.61480913	0.437908312	3.09340554	0
|| LUM || Lumican || Hs.406475 || 102662	1	3.638690565	2.41116296	0.662645784	3.40779244	0
|| HSPC159 || HSPC159 protein || Hs.372208	1	3.558899335	1.60042407	0.449696359	3.27038842	0
|| LUM || Lumican || Hs.406475 || 110722	1	3.541719272	2.29288889	0.647394306	2.86473787	0
|| OMD || Osteomodulin || Hs.94070 || 114768	1	3.535697485	1.62297685	0.459025937	3.02783159	0
|| || || 114871	1	3.509166045	2.16945556	0.618225392	3.47891429	0
|| IGF1 || Insulin-like growth factor 1 (somatom	1	3.49570566	1.57951799	0.451845248	3.51097942	0
|| BCHE || Butyrylcholinesterase || Hs.420483	1	3.458963521	2.03993783	0.589754075	8.19084838	0
|| TGFBR2 || Transforming growth factor, beta	1	3.438660607	1.97616204	0.574689469	3.56641801	0
|| SOX5 || SRY (sex determining region Y)-bo	1	3.413685036	1.93384259	0.566497076	3.92246288	0
|| ARGBP2 || Sorbin and SH3 domain contain	1	3.375596872	2.24805053	0.665971268	2.41323567	0
|| RASSF2 || Ras association (RalGDS/AF-6)	1	3.363037447	1.51283333	0.449841358	2.6661658	0
|| MRE11A || MRE11 meiotic recombination 1	1	3.360484562	1.45137484	0.431894512	2.55488429	0
|| TM4SF1 || Transmembrane 4 L six family m	1	3.339574713	1.59829444	0.478592211	2.65659715	0
|| LAMA4 || Laminin, alpha 4 || Hs.213861 || 1	1	3.338171702	1.63975802	0.491214404	2.83557883	0
|| AOC3 || Amine oxidase, copper containing	1	3.333153788	1.45409848	0.436253042	2.59675707	0
|| SIAT10 || ST3 beta-galactoside alpha-2,3-si	1	3.326431076	2.04631728	0.615169002	3.4291595	0
|| DSCR1L1 || Down syndrome critical region	1	3.300972344	1.61077672	0.487970377	2.83995666	0
|| APOD || Apolipoprotein D || Hs.522555 || 10	1	3.29272151	2.84420231	0.863784655	2.75957315	0
|| CYP1B1 || Cytochrome P450, family 1, sub	1	3.286552521	2.38707407	0.726315511	3.82091006	0
|| AD031 || AD031 protein || Hs.44004 || 3170	1	3.276640796	1.46332407	0.446592765	2.75235183	0
|| THBD || Thrombomodulin || Hs.2030 || 9859	1	3.267356009	1.43309676	0.438610533	2.62612859	0
|| ADAMTS1 || ADAM metallopeptidase with t	1	3.254769201	1.54590506	0.474966107	3.1826151	0
|| CYP1B1 || Cytochrome P450, family 1, sub	1	3.249250477	1.91551667	0.589525701	3.52854608	0
|| APOD || Apolipoprotein D || Hs.522555 || 10	1	3.248499027	2.21792593	0.682754068	2.51354394	0
|| || Transcribed locus || Hs.247150 || 119666	1	3.246954485	1.91940741	0.591140842	2.96701383	0
|| TNFSF10 || Tumor necrosis factor (ligand) s	1	3.245061059	1.58168342	0.48741253	2.69025679	0
|| || Transcribed locus || Hs.560535 || 107090	1	3.210248831	1.66014815	0.517140021	3.93922443	0
|| ALDH1A3 || Aldehyde dehydrogenase 1 fam	1	3.191025506	1.79035185	0.561058459	3.65989277	0
|| RALGPS2 || Ral GEF with PH domain and	1	3.189402776	1.54962037	0.485865373	2.4588726	0
|| GPA33 || Glycoprotein A33 (transmembrane	1	3.178911735	1.48168071	0.466096839	3.39184294	0
|| CMAH || Cytidine monophosphate-N-acetyln	1	3.177191844	1.47846759	0.465337841	2.70329248	0
|| SIAT10 || ST3 beta-galactoside alpha-2,3-si	1	3.151065365	1.74836111	0.554847618	3.12654065	0
|| ADAMTS1 || ADAM metallopeptidase with t	1	3.116508135	1.73102381	0.555436962	3.37394641	0
|| OSTM1 || Osteopetrosis associated transm	1	3.097085332	1.33229558	0.430177226	2.32705214	0
|| STK17A || Serine/threonine kinase 17a (apo	1	3.095482441	1.31496049	0.424799856	2.71128593	0
|| CFH || Complement factor H || Hs.363396 ||	1	3.080627131	1.74108208	0.565171312	2.30371616	0

Table 1c

Row	Gene ID	Gene Nar	Score(d)	Numerator(r	Denominator(s+s0)	Fold Change	q-value(%)
4704	|| SERPINA5 || Serpin	1	6.004949059	3.72711249	0.620673456	15.4244079	0
4703	|| SERPINA5 || Serpin	1	5.676090819	3.36553312	0.592931513	12.642694	0
5263	|| MAL || Mal, T-cell dif	1	4.793000991	3.77839161	0.788314381	7.073874	0
329	|| SLC15A3 || Solute c	1	4.768834072	2.43471204	0.510546605	4.92570351	0
4988	|| APOC2 || Apolipopro	1	4.763704629	3.4394258	0.722006519	5.00166363	0
5264	|| || Transcribed locus	1	4.609618204	3.3866573	0.734693667	5.28829885	0
5156	|| CTNNAL1 || Catenin	1	4.555031264	2.84420979	0.624410597	4.56085308	0
412	|| SLC2A5 || Solute ca	1	4.478826003	3.09964216	0.692065768	4.83704532	0
4977	|| ANK3 || Ankyrin 3, n	1	4.442590053	2.85613559	0.642898749	5.12824732	0
4987	|| APCS || Amyloid P c	1	4.282614836	2.45367855	0.572939349	3.99470135	0
5265	|| PCOLN3 || Procollag	1	4.204916561	2.85560315	0.679110538	5.3145688	0
4978	|| || || 115174	1	4.201732093	2.5764347	0.613183954	4.59519355	0
4986	|| ALOX5AP || Arachid	1	4.180881601	2.74828105	0.657344865	4.22120786	0
411	|| HLA-DRB5 || Major h	1	4.076986198	2.15998776	0.529800116	3.43376649	0
5261	|| LOC286191 || Hypotl	1	4.044751599	2.55327209	0.631255598	4.67333867	0
5260	|| RPESP || RPE-spon	1	4.001363666	2.25392033	0.563288048	4.10764883	0
5262	|| L1CAM || L1 cell adh	1	3.995710183	3.16762448	0.792756314	4.71111161	0
404	|| HLA-DRB5 || **Major	1	3.9708283	2.25247173	0.567254879	3.67641568	0
4979	|| ANK3 || Ankyrin 3, n	1	3.95383411	2.55599524	0.64645991	4.55382756	0
414	|| RASSF4 || Ras assc	1	3.886845201	2.13090482	0.548235061	3.59405996	0
5134	|| SIAT7B || ST6 (alpha	1	3.882142988	2.84759441	0.733510954	3.44583927	0
359	|| RAB20 || RAB20, me	1	3.860581424	1.84690117	0.478399744	3.39837851	0
5114	|| SOX10 || SRY (sex d	1	3.842512751	3.20823341	0.834931103	2.92161566	0
429	|| FEZ1 || Fasciculatior	1	3.841767155	1.78518963	0.464679288	3.13038672	0
5255	|| CRYAB || Crystallin,	1	3.839845731	2.72711906	0.710215789	3.93775379	0
5259	|| FLJ14525 || Hypothe	1	3.830032639	1.96455754	0.512934934	3.35821422	0
372	|| APOC1 || Apolipopro	1	3.829958868	2.59238462	0.676870093	3.31288185	0
4701	|| CDH2 || Cadherin 2,	1	3.819404209	2.30206056	0.60272766	4.08702312	0
4696	|| MAP1B || Microtubul	1	3.803994797	1.89594246	0.498408269	3.27861955	0
386	|| MS4A7 || Membrane	1	3.79206023	2.07331923	0.546752715	3.76365393	0
4705	|| C10orf45 || Chromos	1	3.78417288	2.01348679	0.53208108	3.62430799	0
4976	|| SORCS1 || Sortilin-re	1	3.778582031	2.80474522	0.742274535	3.23383023	0
389	|| VMD2 || Vitelliform m	1	3.755890899	2.09299767	0.557257313	3.19543441	0
403	|| HLA-DRB1 || Major h	1	3.749667044	2.0737798	0.553057051	3.15795577	0
4971	|| KCNMB4 || Potassiu	1	3.745622326	2.26450155	0.604572847	4.23002216	0
1135	|| EPB41L4B || Erythrc	1	3.739550356	2.22678516	0.595468694	5.1477026	0
405	|| HLA-DRB1 || Major h	1	3.721375543	2.28107366	0.612965188	2.96282595	0
488	|| MT1K || Metallothion	1	3.708932185	1.93780342	0.522469358	4.25537481	0
5257	|| SPTBN1 || Spectrin,	1	3.706913477	2.11531119	0.570639483	3.49559244	0
410	|| HLA-DRB1 || Major h	1	3.704294151	1.93705393	0.522921196	3.30765227	0
371	|| APOC1 || Apolipopro	1	3.699234789	2.48006488	0.670426459	3.11366049	0
4697	|| MS4A8B || Membrar	1	3.691777637	1.75859091	0.476353422	3.26621262	0
5115	|| SNCA || Synuclein, a	1	3.691175466	2.87982867	0.78019284	3.5942503	0

Table 1d

Gene ID	Gene Nar	Score(d)	Numerator(r	Denominator(s+s0)	Fold Change	q-value(%)
|| SSX1 || Synovial sarcoma, X breakpoint 1 || Hs.43	1	7.587880343	3.99983325	0.527134465	11.4705629	0
|| ZIC2 || Zic family member 2 (odd-paired homolog,	1	5.647026249	4.04358187	0.716055086	23.9644481	0
|| EFNB3 || Ephrin-B3 || Hs.26988 || 103884	1	5.148958369	3.33042946	0.646816156	7.79849705	0
|| SIX4 || Sine oculis homeobox homolog 4 (Drosoph	1	4.676161329	3.32675693	0.711429032	6.97722991	0
|| CRABP2 || Cellular retinoic acid binding protein 2	1	4.63261851	3.45109148	0.744954817	6.511293	0
|| TGFB2 || Transforming growth factor, beta 2 || Hs.	1	4.50245711	3.05007999	0.677425663	6.30330369	0
|| CRABP2 || Cellular retinoic acid binding protein 2	1	4.486542954	2.72729975	0.607884462	5.37323988	0
|| CA14 || Carbonic anhydrase XIV || Hs.528988 || 22	1	4.440070067	3.03882291	0.684408774	9.48300046	0
|| COL4A5 || Collagen, type IV, alpha 5 (Alport synd	1	4.334618239	2.85740515	0.659205722	6.51321094	0
|| MSX2 || Msh homeo box homolog 2 (Drosophila) |	1	4.33384269	3.15208153	0.727317937	11.1305882	0
|| EGFL3 || EGF-like-domain, multiple 3 || Hs.56186	1	4.116669843	2.44159999	0.593100754	4.33070308	0
|| || || || 319147	1	4.086960689	2.68038958	0.655839334	8.62519096	0
|| || || || 106113	1	4.074052302	2.41630268	0.593095647	6.70830919	0
|| ENC1 || Ectodermal-neural cortex (with BTB-like d	1	3.999189769	2.2361502	0.559150809	4.77580628	0
|| ENC1 || Ectodermal-neural cortex (with BTB-like d	1	3.941565627	2.91637214	0.739901962	6.83013292	0
|| TLE1 || Transducin-like enhancer of split 1 (E(sp1)	1	3.933089616	1.96836848	0.500463674	3.62235235	0
|| FZD1 || Frizzled homolog 1 (Drosophila) || Hs.942	1	3.900561186	2.61420493	0.670212516	5.47643838	0
|| WNT5A || Wingless-type MMTV integration site fa	1	3.883754141	2.46655535	0.635095648	4.26568077	0
|| SHANK2 || SH3 and multiple ankyrin repeat doma	1	3.872202089	2.45165092	0.633141262	6.19380079	0
|| MSX2 || Msh homeo box homolog 2 (Drosophila) |	1	3.839887634	2.90608712	0.756815666	8.396491	0
|| HSRG1 || MON1 homolog B (yeast) || Hs.513743	1	3.81923571	2.4376584	0.638258171	13.0023622	0
|| NXN || **Nucleoredoxin || Hs.527989 || 99548	1	3.814806952	2.32950986	0.610649474	4.74055278	0
|| EBPL || Emopamil binding protein-like || Hs.43327	1	3.768695546	1.78197505	0.472836033	3.14161052	0
|| TACSTD1 || Tumor-associated calcium signal tran	1	3.748359159	3.02219536	0.806271552	26.4938469	0
|| TMEM30B || Transmembrane protein 30B || Hs.14	1	3.697434778	2.47869531	0.67038243	5.3271336	0
|| TLE4 || Transducin-like enhancer of split 4 (E(sp1)	1	3.685344091	1.90286449	0.516332925	3.86286493	0
|| FOXD1 || Forkhead box D1 || Hs.519385 || 101053	1	3.673260968	2.28149261	0.621108227	4.26885681	0
|| MLLT3 || Myeloid/lymphoid or mixed-lineage leuke	1	3.660170485	2.38412971	0.651371218	5.02421071	0
|| CRABP1 || Cellular retinoic acid binding protein 1	1	3.649427519	3.21280794	0.880359434	4.124915	0
|| TACSTD1 || Tumor-associated calcium signal tran	1	3.64715627	3.04224236	0.834140939	23.6065738	0
|| FOXC1 || Forkhead box C1 || Hs.348883 || 120223	1	3.63808051	1.83013909	0.50305074	3.28205873	0
|| COL27A1 || Collagen, type XXVII, alpha 1 || Hs.49	1	3.631422802	1.91954262	0.528592435	3.97011589	0
|| LOC152485 || Hypothetical protein LOC152485 || I	1	3.604161901	2.15574047	0.598125315	3.38293195	0
|| ZNF423 || Zinc finger protein 423 || Hs.530930 || 3(	1	3.588203165	2.06748531	0.57618959	3.49184109	0
|| CRA || Myotubularin related protein 11 || Hs.42514	1	3.580370696	1.74973832	0.488703117	3.69298999	0
|| AUTS2 || Autism susceptibility candidate 2 || Hs.2	1	3.574285204	1.81889804	0.508884417	3.08987294	0
|| PRAME || Preferentially expressed antigen in mel	1	3.567577233	1.8957265	0.531376442	2.89064963	0
|| ITM2C || Integral membrane protein 2C || Hs.1115	1	3.540345798	1.77246385	0.500647098	3.3639521	0
|| KIAA0888 || KIAA0888 protein || Hs.91662 || 1112	1	3.529635959	2.1879862	0.619890046	4.21348176	0
|| C1orf9 || Chromosome 1 open reading frame 9 || H	1	3.522497804	2.28997606	0.650100068	7.46953531	0
|| MTERF || Mitochondrial transcription termination f	1	3.52186333	2.00955935	0.570595495	5.25364604	0
|| AXIN2 || Axin 2 (conductin, axil) || Hs.156527 || 30	1	3.516936933	1.90479454	0.541606113	3.06175147	0
|| MYO9B || Myosin IXB || Hs.123198 || 104290	1	3.489518058	2.07132559	0.593585005	4.47507892	0
|| FZD1 || Frizzled homolog 1 (Drosophila) || Hs.942	1	3.481759896	2.32872728	0.668836264	4.89941014	0
|| FGFR3 || Fibroblast growth factor receptor 3 (acho	1	3.472690014	1.68659252	0.485673213	4.07241832	0

Table 2

Gene Set	SIZE	ES	NES	NOM p-value
SIG_PIP3_signaling_in_B_lymphocytes	36	0.539579	1.68401	0.035714
ST_Tumor_Necrosis_Factor_Pathway	27	0.533768	1.607012	0.025341
TGF_Beta_Signaling_Pathway	41	0.445959	1.518109	0.034417
cell_surface_receptor_linked_signal_transduction	73	0.428377	1.515348	0.069565
ST_JNK_MAPK_Pathway	49	0.483808	1.505573	0.016667
G13_Signaling_Pathway	26	0.510994	1.491692	0.009542
NFKB_INDUCED	91	0.39855	1.488427	0.068136
ST_Fas_Signaling_Pathway	45	0.386641	1.459184	0.014706
Met Pathway	51	0.473679	1.445063	0.078671

Table 3a

TGFB signaling pathway

PROBE	GENE SYMBOL	GENE_TITLE	RANK IN GENE LIST	CORE_ENRICHMENT
IMAGE:841149	TGFBR2	transforming growth factor, beta receptor II (70/80kDa)	14	Yes
IMAGE:824109	ZFHX1B	zinc finger homeobox 1b	26	Yes
IMAGE:429042	THBS1	thrombospondin 1	673	Yes
IMAGE:364194	SKIL	SKI-like	777	Yes
IMAGE:767844	MADH2	MAD, mothers against decapentaplegic homolog 2 (Drosophila)	868	Yes
IMAGE:726035	JUN	v-jun sarcoma virus 17 oncogene homolog (avian)	1095	Yes
IMAGE:824193	TGFBR1	transforming growth factor, beta receptor I	1170	Yes
IMAGE:774754	CTNNB1	catenin (cadherin-associated protein), beta 1, 88kDa	1354	Yes
IMAGE:282838	ZFHX1B	zinc finger homeobox 1b	1357	Yes
IMAGE:840691	STAT1	signal transducer and activator of transcription 1, 91kDa	1392	Yes
IMAGE:26474	FOS	v-fos FBJ murine osteosarcoma viral oncogene homolog	1457	Yes
IMAGE:788421	MADH4	MAD, mothers against decapentaplegic homolog 4 (Drosophila)	1618	Yes
IMAGE:269425	ZFHX1B	zinc finger homeobox 1b	1696	Yes
IMAGE:358531	JUN	v-jun sarcoma virus 17 oncogene homolog (avian)	1702	Yes
IMAGE:280356	MADH2	MAD, mothers against decapentaplegic homolog 2 (Drosophila)	1803	Yes
IMAGE:269269	TGFBR3	transforming growth factor, beta receptor III (betaglycan, 300kDa)	2188	Yes
IMAGE:23275	MADH4	MAD, mothers against decapentaplegic homolog 4 (Drosophila)	2366	Yes
IMAGE:545503	STAT1	signal transducer and activator of transcription 1, 91kDa	2501	Yes
IMAGE:1883559	FST	follistatin	2574	Yes

ST_Tumor_Necrosis_Factor_Pathway

PROBE	GENE SYMBOL	GENE_TITLE	RANK IN GENE LIST	CORE_ENRICHMENT
IMAGE:813671	HRB	HIV-1 Rev binding protein	60	Yes
IMAGE:813714	CFLAR	CASP8 and FADD-like apoptosis regulator	491	Yes
IMAGE:34852	BIRC2	baculoviral IAP repeat-containing 2	717	Yes
IMAGE:272632	NR2C2	nuclear receptor subfamily 2, group C, member 2	814	Yes
IMAGE:309776	CFLAR	CASP8 and FADD-like apoptosis regulator	850	Yes
IMAGE:299468	NR2C2	nuclear receptor subfamily 2, group C, member 2	893	Yes
IMAGE:51921	BAG4	BCL2-associated athanogene 4	981	Yes
IMAGE:726035	JUN	v-jun sarcoma virus 17 oncogene homolog (avian)	1095	Yes
IMAGE:279974	NR2C2	nuclear receptor subfamily 2, group C, member 2	1277	Yes
IMAGE:358531	JUN	v-jun sarcoma virus 17 oncogene homolog (avian)	1702	Yes
IMAGE:127032	BIRC3	baculoviral IAP repeat-containing 3	1853	Yes
IMAGE:2508563	TNFAIP3	tumor necrosis factor, alpha-induced protein 3	3080	Yes
IMAGE:796134	MAP3K7	mitogen-activated protein kinase kinase kinase 7	3648	Yes
IMAGE:843319	HRB	HIV-1 Rev binding protein	3789	Yes
IMAGE:429574	CASP3	caspase 3, apoptosis-related cysteine protease	3837	Yes

Table 3b

Cell_surface_receptor_linked_signal_transduction

PROBE	GENE SYMBOL	GENE_TITLE	RANK IN GENE LIST	CORE_ENRICHMENT
IMAGE:49665	EDNRB	endothelin receptor type B	10	Yes
IMAGE:768246	PRKCA	protein kinase C, alpha	149	Yes
IMAGE:208718	ANXA1	annexin A1	203	Yes
IMAGE:768452	C21orf4	chromosome 21 open reading frame 4	264	Yes
IMAGE:503741	LIFR	leukemia inhibitory factor receptor	287	Yes
IMAGE:208001	CD59	CD59 antigen p18-20	305	Yes
IMAGE:782812	IFNAR1	interferon (alpha, beta and omega) receptor 1	423	Yes
IMAGE:204897	PLCG2	phospholipase C, gamma 2 (phosphatidylinositol-specific)	608	Yes
IMAGE:271050	EDNRB	endothelin receptor type B	657	Yes
IMAGE:897821	IL13RA1	interleukin 13 receptor, alpha 1	661	Yes
IMAGE:34852	BIRC2	baculoviral IAP repeat-containing 2	717	Yes
IMAGE:141931	BAIAP1	BAI1-associated protein 1	921	Yes
IMAGE:46694	LIFR	leukemia inhibitory factor receptor	1091	Yes
IMAGE:229365	PTPRC	protein tyrosine phosphatase, receptor type, C	1201	Yes
IMAGE:108837	CCL2	chemokine (C-C motif) ligand 2	1411	Yes
IMAGE:295889	LIFR,SHMT2	serine hydroxymethyltransferase 2 (mitochondrial)leukemia inhibitory factor receptor	1498	Yes
IMAGE:146671	IL1R1	interleukin 1 receptor, type I	1514	Yes
IMAGE:435470	PDGFA	platelet-derived growth factor alpha polypeptide	1518	Yes
IMAGE:841238	IL7R	interleukin 7 receptor	1685	Yes
IMAGE:2471879	PTPRC	protein tyrosine phosphatase, receptor type, C	1694	Yes
IMAGE:190887	MYD88	myeloid differentiation primary response gene (88)	1749	Yes
IMAGE:127032	BIRC3	baculoviral IAP repeat-containing 3	1853	Yes
IMAGE:768561	CCL2	chemokine (C-C motif) ligand 2	1871	Yes
IMAGE:2514377	BRD8	bromodomain containing 8	1907	Yes
IMAGE:785575	IFNGR2	interferon gamma receptor 2 (interferon gamma transducer 1)	1916	Yes
IMAGE:298402	CSNK1A1	Homo sapiens mRNA; cDNA DKFZp779B1535 (from clone DKFZp779B1535)casein kinase 1, alpha 1	2115	Yes
IMAGE:704459	CD69	CD69 antigen (p60, early T-cell activation antigen)	2162	Yes
IMAGE:201890	BIRC3	baculoviral IAP repeat-containing 3	2229	Yes
IMAGE:501431	LIFR	leukemia inhibitory factor receptor	2262	Yes
IMAGE:753743	IL6ST	interleukin 6 signal transducer (gp130, oncostatin M receptor)	2346	Yes
IMAGE:428231	BIRC3	baculoviral IAP repeat-containing 3	2537	Yes
IMAGE:687592	OSMR	oncostatin M receptor	2559	Yes
IMAGE:433490	CSNK1A1	casein kinase 1, alpha 1	2657	Yes

Table 3c

JNK_MAPK_Pathway

PROBE	GENE SYMBOL	GENE_TITLE	RANK IN GENE LIST	CORE_ENRICHMENT
IMAGE:199624	GAB1	GRB2-associated binding protein 1	19	Yes
IMAGE:593306	MAP3K1	mitogen-activated protein kinase kinase kinase 1	47	Yes
IMAGE:838692	MAP3K7IP2	mitogen-activated protein kinase kinase kinase 7 interacting protein 2	501	Yes
IMAGE:810230	MAP3K1	mitogen-activated protein kinase kinase kinase 1	655	Yes
IMAGE:119133	MAPK8	mitogen-activated protein kinase 8	711	Yes
IMAGE:272632	NR2C2	nuclear receptor subfamily 2, group C, member 2	814	Yes
IMAGE:726035	JUN	v-jun sarcoma virus 17 oncogene homolog (avian)	1095	Yes
IMAGE:279974	NR2C2	nuclear receptor subfamily 2, group C, member 2	1277	Yes
IMAGE:140337	PAPPA	pregnancy-associated plasma protein A	1373	Yes
IMAGE:1565455	NR2C2	nuclear receptor subfamily 2, group C, member 2	1382	Yes
IMAGE:588550	TRAF6	TNF receptor-associated factor 6	1478	Yes
IMAGE:146671	IL1R1	interleukin 1 receptor, type I	1514	Yes
IMAGE:50765	ATF2	activating transcription factor 2	1538	Yes
IMAGE:176565	MAP3K2	mitogen-activated protein kinase kinase kinase 2	1616	Yes
IMAGE:358531	JUN	v-jun sarcoma virus 17 oncogene homolog (avian)	1702	Yes
IMAGE:854746	CDC42	cell division cycle 42 (GTP binding protein, 25kDa)	1728	Yes
IMAGE:41333	MAP3K2	mitogen-activated protein kinase kinase kinase 2	1780	Yes
IMAGE:1880757	MAP3K5	mitogen-activated protein kinase kinase kinase 5	1983	Yes
IMAGE:1470508	MAPK8	mitogen-activated protein kinase 8	2203	Yes
IMAGE:123087	PAPPA	pregnancy-associated plasma protein A	2347	Yes
IMAGE:813648	DLD	dihydrolipoamide dehydrogenase	2534	Yes
IMAGE:365531	CDC42	cell division cycle 42 (GTP binding protein, 25kDa)	2569	Yes
IMAGE:129112	PAPPA	pregnancy-associated plasma protein A	2812	Yes

Table 3d

NFKB_induced signaling pathway

PROBE	GENE SYMBOL	GENE_TITLE	RANK IN GENE LIST	CORE_ENRICHMENT
IMAGE:25154	PLAT	suppressor of S. cerevisiae gcr2plasminogen activator, tissue	48	Yes
IMAGE:2545220	RABEP1	rabaptin, RAB GTPase binding effector protein 1	97	Yes
IMAGE:261246	SPTBN1	spectrin, beta, non-erythrocytic 1	107	Yes
IMAGE:280444	KIAA0608	KIAA0608 protein	247	Yes
IMAGE:701112	XPC	xeroderma pigmentosum, complementation group C	485	Yes
IMAGE:813714	CFLAR	CASP8 and FADD-like apoptosis regulator	491	Yes
IMAGE:489729	ETS1	v-ets erythroblastosis virus E26 oncogene homolog 1 (avian)	548	Yes
IMAGE:840708	SOD2	superoxide dismutase 2, mitochondrial	653	Yes
IMAGE:841332	ARHGDIB	Rho GDP dissociation inhibitor (GDI) beta	671	Yes
IMAGE:78148	SOD2	superoxide dismutase 2, mitochondrial	792	Yes
IMAGE:530185	CD83	CD83 antigen (activated B lymphocytes, immunoglobulin superfamily)	839	Yes
IMAGE:309776	CFLAR	CASP8 and FADD-like apoptosis regulator	850	Yes
IMAGE:857002	PNRC1	proline-rich nuclear receptor coactivator 1	985	Yes
IMAGE:2371739	SPTBN1	spectrin, beta, non-erythrocytic 1	1023	Yes
IMAGE:727251	CD9	CD9 antigen (p24)	1033	Yes
IMAGE:712559	SEC24A	SEC24 related gene family, member A (S. cerevisiae)	1209	Yes
IMAGE:108837	CCL2	chemokine (C-C motif) ligand 2	1411	Yes
IMAGE:784593	ARHE	ras homolog gene family, member E	1653	Yes
IMAGE:841238	IL7R	interleukin 7 receptor	1685	Yes
IMAGE:240651	UTX	ubiquitously transcribed tetratricopeptide repeat gene, X chromosome	1724	Yes
IMAGE:296556	FN1	fibronectin 1	1834	Yes
IMAGE:768561	CCL2	chemokine (C-C motif) ligand 2	1871	Yes
IMAGE:137296	SEC24A	SEC24 related gene family, member A (S. cerevisiae)	1938	Yes
IMAGE:321816	TNFAIP2	tumor necrosis factor, alpha-induced protein 2	1969	Yes
IMAGE:324383	FGF2	fibroblast growth factor 2 (basic)	2159	Yes
IMAGE:841008	GBP1	guanylate binding protein 1, interferon-inducible, 67kDa	2340	Yes
IMAGE:753587	BTN3A3	butyrophilin, subfamily 3, member A3	2398	Yes
IMAGE:489025	RAC1	ras-related C3 botulinum toxin substrate 1 (rho family, small GTP binding protein Rac1)	2438	Yes
IMAGE:415851	ARHE	ras homolog gene family, member E	2586	Yes
IMAGE:898332	NPR1	natriuretic peptide receptor A/guanylate cyclase A (atrionatriuretic peptide receptor A)	2832	Yes
IMAGE:878449	MAP1B	microtubule-associated protein 1B	2923	Yes
IMAGE:2404494	SEC24A	SEC24 related gene family, member A (S. cerevisiae)	3100	Yes
IMAGE:357031	TNFAIP6	tumor necrosis factor, alpha-induced protein 6	3117	Yes
IMAGE:768316	ABCC1	ATP-binding cassette, sub-family C (CFTR/MRP), member 1chromosome condensation 1-like	3141	Yes
IMAGE:664121	LITAF	lipopolysaccharide-induced TNF factor	3218	Yes
IMAGE:346860	SOD2	superoxide dismutase 2, mitochondrial	3283	Yes
IMAGE:813614	SPRR1B	small proline-rich protein 1B (cornifin)	3488	Yes
IMAGE:186132	SELE	selectin E (endothelial adhesion molecule 1)	3504	Yes

Table 3e

Met Pathway

PROBE	GENE SYMBOL	GENE_TITLE	RANK IN GENE LIST	CORE_ENRICHMENT
IMAGE:199624	GAB1	GRB2-associated binding protein 1	19	Yes
IMAGE:1925760	PTEN	phosphatase and tensin homolog (mutated in multiple advanced cancers 1)	65	Yes
IMAGE:704905	RAP1A	RAP1A, member of RAS oncogene family	221	Yes
IMAGE:814776	PTPN11	protein tyrosine phosphatase, non-receptor type 11 (Noonan syndrome 1)	331	Yes
IMAGE:366966	PTEN	phosphatase and tensin homolog (mutated in multiple advanced cancers 1)	345	Yes
IMAGE:502527	ITGA1	integrin, alpha 1	454	Yes
IMAGE:345430	PIK3CA	phosphoinositide-3-kinase, catalytic, alpha polypeptide	600	Yes
IMAGE:119133	MAPK8	mitogen-activated protein kinase 8	711	Yes
IMAGE:724892	PTK2	PTK2 protein tyrosine kinase 2	1007	Yes
IMAGE:276639	Hs.350524,RASA1	RAS p21 protein activator (GTPase activating protein) 1Homo sapiens mRNA; cDNA DKFZp566M223 (from clone DKFZp566M223)	1009	Yes
IMAGE:726035	JUN	v-jun sarcoma virus 17 oncogene homolog (avian)	1095	Yes
IMAGE:626841	MET	met proto-oncogene (hepatocyte growth factor receptor)	1207	Yes
IMAGE:26474	FOS	v-fos FBJ murine osteosarcoma viral oncogene homolog	1457	Yes
IMAGE:970590	MAPK1	mitogen-activated protein kinase 1	1536	Yes
IMAGE:785530	ITGA1	integrin, alpha 1	1667	Yes
IMAGE:358531	JUN	v-jun sarcoma virus 17 oncogene homolog (avian)	1702	Yes
IMAGE:322160	PTEN	phosphatase and tensin homolog (mutated in multiple advanced cancers 1)	1827	Yes
IMAGE:452423	SOS1	son of sevenless homolog 1 (Drosophila)	1950	Yes
IMAGE:897961	RAP1B	RAP1B, member of RAS oncogene family	2029	Yes
IMAGE:325953	ITGB1	integrin, beta 1 (fibronectin receptor, beta polypeptide, antigen CD29 includes MDF2, MSK12)	2063	Yes
IMAGE:1470508	MAPK8	mitogen-activated protein kinase 8	2203	Yes
IMAGE:34773	PTPN11	protein tyrosine phosphatase, non-receptor type 11 (Noonan syndrome 1)	2269	Yes
IMAGE:39808	PIK3R1	phosphoinositide-3-kinase, regulatory subunit, polypeptide 1 (p85 alpha)	2503	Yes
IMAGE:343072	ITGB1	integrin, beta 1 (fibronectin receptor, beta polypeptide, antigen CD29 includes MDF2, MSK12)	2560	Yes
IMAGE:321189	RAP1B	RAP1B, member of RAS oncogene family	2568	Yes

APPENDICES

1. AACR 2006 abstract
2. Copy of manuscript in press in The American Journal of Surgical Pathology.

American Association for Cancer Research (AACR) 2006 annual meeting abstract.

Genome-wide transcriptome analysis of nerve sheath tumors

Subbaya Subramanian[1], Robert B. West[1], Torsten O. Nielsen[2], Brian P. Rubin[3], Erinn Downs-Kelly[4], John R. Goldblum[4], Shirley Zhu[1], Kelli Montgomery[1], Pancras C.W Hogendoorn[5], Christopher L. Corless[6], Andre M. Oliveira[7], Christopher D.M. Fletcher[8], Matt van de Rijn[1]

[1]Department of Pathology, Stanford University Medical Center, Stanford, California, USA;
[2]Department of Pathology, Vancouver General Hospital, Vancouver, British Columbia, Canada;
[3]Department of Anatomic Pathology, University of Washington Medical Center, Seattle, Washington, USA;
[4]Department of Anatomic Pathology, Cleveland Clinic Foundation, Cleveland, Ohio, USA;
[5]Department of Pathology, Leiden University Medical Center, The Netherlands;
[6]Department of Pathology, Oregon Health and Science University, Portland, Oregon, USA;
[7]Department of Laboratory Medicine and Pathology, Mayo Clinic, Rochester, Minnesota, USA;
[8]Department of Pathology, Brigham and Women's hospital and Harvard Medical School, Boston, Massachusetts, USA.

Malignant peripheral nerve sheath tumors (MPNSTs) are aggressive soft tissue tumors that arise from neurofibromas in patients with neurofibromatosis but also occur sporadically. Malignant transformation is a life threatening complication in patients with neurofibromatosis. The transformation of neurofibromas into MPNSTs is not completely understood at a molecular level. The goal of this study is to identify genes that will serve as molecular markers for progression of neurofibroma to MPNST, and to identify novel potential therapeutic targets. Gene expression profiling using 43000 spot cDNA microarrays was performed on 32 cases of MPNSTs, 23 schwannomas, 20 neurofibromas and 16 synovial sarcomas. Using unsupervised hierarchical clustering, most tumors grouped together according to tumor type. There appear to be at least two subtypes of MPNSTs. Analysis employing 'significance analysis of microarrays' identified genes that were differentially expressed in various nerve sheath tumors. A major trend in transformation from neurofibroma towards MPNST is accompanied by the loss of expression of a large number of genes, rather than widespread *de novo* increase in gene expression upon transformation. *NF1* is one of the genes for which loss of expression was noticed in most of the MPNSTS. Potential signaling pathways were identified using 'Gene Set Enrichment Analysis' method. The expression of genes associated with MET and TFGB signaling pathways in the majority of neurofibromas, but not in MPNST, suggest that these pathways are affected during malignant transformation. A detailed list of genes and the signaling pathways that are associated with various nerve sheath tumors will be discussed.

Editorial Manager(tm) for American Journal of Surgical Pathology
Manuscript Draft

Manuscript Number: AJSP-D-06-00227R1

Title: TLE1 AS A DIAGNOSTIC IMMUNOHISTOCHEMICAL MARKER FOR SYNOVIAL SARCOMA EMERGING FROM GENE EXPRESSION PROFILING STUDIES

Article Type: Original Article

Section/Category:

Keywords: Synovial sarcoma; TLE; immunohistochemistry; microarray; expression profiling.

Corresponding Author: Dr. Torsten O. Nielsen, MD/PhD

Corresponding Author's Institution: University of British Columbia

First Author: Jefferson Terry, MD

Order of Authors: Jefferson Terry, MD; Tsuyoshi Saito , MD/PhD; Subbaya Subramanian, PhD; Cindy Ruttan, MSc; Cristina R Antonescu, MD; John R Goldblum, MD; Erinn Downs-Kelly, MD; Christopher L Corless, MD/PhD; Brian P Rubin, MD/PhD; Matt van de Rijn, MD/PhD; Marc Ladanyi, MD; Torsten O Nielsen, MD/PhD

Manuscript Region of Origin:

Abstract: Synovial sarcoma is a soft tissue malignancy defined by the SYT-SSX fusion oncogene. Demonstration of the t(X;18) by cytogenetics, FISH or RT-PCR has become the gold standard for diagnosis, but practical considerations limit the availability of these methods. Gene expression profiling studies performed by several independent groups have consistently identified TLE1 as an excellent discriminator of synovial sarcoma from other sarcomas, including histologically similar tumors such as malignant peripheral nerve sheath tumor. TLE proteins (human homologues of groucho) are transcriptional corepressors that inhibit Wnt signaling and other cell fate determination signals, and so have an established role in repressing differentiation. We examined the expression of TLE proteins in synovial sarcoma and in a broad range of mesenchymal tumors using tissue microarrays to assess the value of anti-TLE antibodies in the

immunohistochemical confirmation of synovial sarcoma. We demonstrate that TLE expression is a consistent feature of synovial sarcoma using both a well-characterized monoclonal antibody recognizing the TLE family of proteins and a commercially available polyclonal antibody raised against TLE1. Both antibodies gave intense and/or diffuse nuclear staining in 91/94 molecularly-confirmed synovial sarcomas. Moderate staining is occasionally seen in schwannoma and solitary fibrous tumor/hemangiopericytoma. In contrast, TLE staining is detected much less frequently and at lower levels, if at all, in 40 other mesenchymal tumors. Our findings establish TLE as a robust immunohistochemical marker for synovial sarcoma, and may have implications for understanding the biology of synovial sarcoma and for developing experimental therapies for this cancer.

Title: TLE1 AS A DIAGNOSTIC IMMUNOHISTOCHEMICAL MARKER FOR SYNOVIAL SARCOMA EMERGING FROM GENE EXPRESSION PROFILING STUDIES

Authors: Jefferson Terry MD[1], Tsuyoshi Saito MD/PhD[2], Subbaya Subramanian PhD[3], Cindy Ruttan BSc[1], Cristina R Antonescu MD[2], John R Goldblum MD[4], Erinn Downs-Kelly MD[4], Christopher L Corless MD/PhD[5], Brian P Rubin MD/PhD[6], Matt van de Rijn MD/PhD[3], Marc Ladanyi MD[2†], Torsten O Nielsen MD/PhD[1†]

[1]Genetic Pathology Evaluation Centre, British Columbia Cancer Agency, 600 West 10th Avenue, Vancouver, BC, Canada V5Z 4E6; [2]Department of Pathology, Memorial Sloan-Kettering Cancer Center, 1275 York Avenue, New York, NY 10021; [3]Department of Pathology, Stanford University Medical Center, 300 Pasteur Drive, Stanford, CA 94305; [4]Department of Anatomic Pathology, Cleveland Clinic, 9500 Euclid Avenue, Cleveland, OH 44195; [5]Department of Pathology and OHSU Cancer Institute, Oregon Health and Science University, Portland, OR 97239-3098; [6]Department of Anatomical Pathology, University of Washington Medical Center, Seattle, WA 98195
† Corresponding authors

Addresses for correspondence and reprint requests:
Torsten O. Nielsen, Anatomical Pathology, Vancouver Coastal Health Research Institute, Room JP1502, 855 West 12th Avenue, Vancouver, British Columbia, Canada, V5Z 1M9. E-mail: torsten@interchange.ubc.ca.
Marc Ladanyi, Department of Pathology, Memorial Sloan-Kettering Cancer Center, 1275 York Avenue, New York, NY 10021. Phone: 212-639-6369; Fax: 212-717-3515; E-mail: ladanyim@mskcc.org.

Sources of support: This research was supported by grants from the Terry Fox Foundation (to T.O.N.), the National Institute of Health (to M.L.), and the U.S. Department of Defense (DoD DAMD17-03-1-0297, to M.V.). T.O.N. is a scholar of the Michael Smith Foundation for Health Research. J.T. is a recipient of a Canadian Institutes of Health Research Doctoral Fellowship. T.S. is a recipient of a postdoctoral fellowship from The Uehara Memorial Foundation (Japan). The Genetic Pathology Evaluation Centre is supported by an unrestricted education grant from Sanofi-Aventis.

Abstract

Synovial sarcoma is a soft tissue malignancy defined by the *SYT-SSX* fusion oncogene. Demonstration of the t(X;18) by cytogenetics, FISH or RT-PCR has become the gold standard for diagnosis, but practical considerations limit the availability of these methods. Gene expression profiling studies performed by several independent groups have consistently identified *TLE1* as an excellent discriminator of synovial sarcoma from other sarcomas, including histologically similar tumors such as malignant peripheral nerve sheath tumor. TLE proteins (human homologues of *groucho*) are transcriptional corepressors that inhibit Wnt signaling and other cell fate determination signals, and so have an established role in repressing differentiation. We examined the expression of TLE proteins in synovial sarcoma and in a broad range of mesenchymal tumors using tissue microarrays to assess the value of anti-TLE antibodies in the immunohistochemical confirmation of synovial sarcoma. We demonstrate that TLE expression is a consistent feature of synovial sarcoma using both a well-characterized monoclonal antibody recognizing the TLE family of proteins and a commercially available polyclonal antibody raised against TLE1. Both antibodies gave intense and/or diffuse nuclear staining in 91/94 molecularly-confirmed synovial sarcomas. Moderate staining is occasionally seen in schwannoma and solitary fibrous tumor/hemangiopericytoma. In contrast, TLE staining is detected much less frequently and at lower levels, if at all, in 40 other mesenchymal tumors. Our findings establish TLE as a robust immunohistochemical marker for synovial sarcoma, and may have implications for understanding the biology of synovial sarcoma and for developing experimental therapies for this cancer.

Key words: Synovial sarcoma, TLE, immunohistochemistry, microarray, expression profiling

Introduction

Synovial sarcoma is a soft tissue malignancy typically occurring in the limbs of young adults, although it may arise at almost any age and anatomic location (10, 11). Synovial sarcomas can be segregated into three histologic subtypes: monophasic, (the most common form, composed entirely of spindle cells), biphasic (displaying both spindle cells and glandular-appearing epithelial components) and poorly differentiated synovial sarcoma (sheets of atypical small blue cells). Morphological variants can also be identified, such as calcifying and fibrous (11), widening the range of appearances and the differential diagnosis. Demonstration in an appropriate histologic context of t(X;18) by cytogenetics, fluorescence *in-situ* hybridization (FISH) or reverse-transcriptase polymerase chain reaction (RT-PCR) is considered the gold standard for the diagnosis of synovial sarcoma; however, several practical issues, including cost and the need for specialized equipment and personnel have limited the use of such diagnostic tests (5, 8). Correct diagnosis of synovial sarcoma based on histology alone can be challenging especially in small biopsies, as monophasic synovial sarcomas can appear similar to other spindle cell tumors (including malignant peripheral nerve sheath tumor (MPNST), fibrosarcoma and hemangiopericytoma), and poorly differentiated synovial sarcomas can resemble several tumor types including Ewing sarcoma. Immunoreactivity for epithelial markers such as cytokeratin and epithelial membrane antigen (EMA) is frequently used to aid in differentiating synovial sarcoma from other spindle cell neoplasms; however, these markers not only lack specificity (12, 27), but also are limited in sensitivity because such epithelial markers are only focally expressed in many synovial sarcomas and are completely negative in a subset of monophasic cases.

The t(X;18) translocation most commonly fuses either the *SSX1* or *SSX2* gene on chromosome X to the *SYT* gene on chromosome 18, resulting in the production of an SYT-SSX fusion protein. The function of SYT-SSX has yet to be fully defined, but combines transcriptional activation (SYT) and repression (SSX) domains and likely drives synovial sarcoma development through dysregulation of gene expression (10, 19). DNA microarray expression profiling, using different platforms, comparison groups and informatics approaches, has consistently shown a major association of the Wnt signaling pathway with synovial sarcoma (1, 3, 14, 20, 21, 25, 29). One prominent gene related to the Wnt pathway is *TLE1*, which has been found to be a good discriminator of synovial sarcoma in multiple studies (Table 1) (3, 20, 23, 29). *TLE1* is one of four *TLE* (*T*ransducin-*L*ike *E*nhancer of split) genes that encode human transcriptional repressors homologous to the *Drosophila* corepressor *groucho* (30); differential overexpression of *TLE2, 3* and *4* has also been demonstrated in synovial sarcoma (1, 3, 25). TLE proteins are temporally expressed in embryogenesis where they are involved in developmental processes including neurogenesis, body patterning and hematopoesis (6, 30, 31, 34). The repressive effect of Groucho and TLE1 is dependent on phosphorylation status and involves histone deacetylase (HDAC) activity (4, 7, 16, 26, 35). The HDAC inhibitor FK228 has recently been shown to inhibit proliferation of synovial sarcoma, supporting the idea that *TLE1* overexpression may play an important role in synovial sarcoma pathobiology and identifying TLE1 as a potential therapeutic target (17, 18).

The specificity of *TLE1* gene expression in synovial sarcoma, particularly when compared to other sarcomas, suggests that TLE1 may be clinically exploitable as an immunohistochemical marker. Here we investigate the protein expression of TLE in synovial sarcoma and in a broad range of mesenchymal neoplasms using tissue microarrays, to assess the value of TLE as a diagnostic marker for this sarcoma.

Materials & Methods

Tumor Samples and Tissue Microarrays

Tissue samples were retrieved from the archives of the Vancouver General Hospital (Vancouver, Canada), Stanford Medical Center (Stanford, CA), University of Washington (Seattle, WA), Cleveland Clinic (Cleveland, OH), Oregon Health & Science University (Portland, OR), and Memorial Sloan-Kettering Cancer Center (MSKCC, New York, NY). Slides corresponding to each archival sample were reviewed by at least two staff pathologists with subspecialty expertise in bone and soft tissue tumors, and representative areas in each original tissue block identified. The TA-19 synovial sarcoma tissue microarray has been previously described (24) and contains 44 molecularly-confirmed synovial sarcomas and 29 other sarcomas with related histologies. The MSKCC synovial sarcoma tissue microarrays contained 52 molecularly-confirmed synovial sarcomas each represented by one 3 mm and one 1 mm core (on different arrays). The TA-138 tissue microarray contains 44 cases of NF-1 related MPNST, 24 sporadic MPNST, 15 synovial sarcomas, 8 localized neurofibroma, 24 plexiform neurofibroma, 11 diffuse neurofibroma, 7 cellular schwannoma, 15 typical schwannoma, 4 perineurioma, 10 melanoma, 5 clear cell carcinoma, and 5 cases of dermatofibrosarcoma protuberans with fibrosarcomatous change. The sarcoma tissue microarrays TA-34 and TA-35 contain 421 benign and malignant soft tissue tumor specimens representing over 50 diagnostic entities and have been previously described (33), as has tissue microarray 03-008, which contains 121 cases of chondroid and osseous tumors (22). For each of these, a tissue microarrayer (Beecher Instruments, MD, USA) was used to extract duplicate 0.6 mm or 1.0 mm cores from representative areas of each original formalin-fixed paraffin-embedded tissue block and to transfer to the recipient microarray block, except for one of the MSKCC tissue microarrays for which 3 mm cores were obtained using a manual punch instrument. All tissue samples were collected according to protocols approved by the ethics committees at the contributing institutions.

Molecular confirmation of synovial sarcoma cases

The presence of t(X;18) in the synovial sarcoma cores and absence of t(X;18) in the non-synovial sarcoma cores with positive TLE staining in the TA-138, 03-008, TA-34 and TA-39 microarrays were verified using a previously described *SYT* breakapart probe FISH method (32). Briefly, a 6 µm section was deparaffinized followed by demasking. Differentially labelled DNA BAC probes were hybridized to the samples overnight and the nuclei counterstained. The TA-19 synovial sarcoma microarray has been previously assessed in this manner (32). Synovial sarcoma cases in which the presence of t(X;18) could not be verified were removed. Cases on the MSKCC tissue microarrays were individually validated by *SYT-SSX* RT-PCR on frozen or

formalin fixed paraffin embedded material, as described previously (2), and included 35 SYT-SSX1 cases and 17 SYT-SSX2 cases.

Immunohistochemistry

Heat-induced epitope retrieval was performed by heating 4 μm sections of each tissue microarray for 30-40 minutes in 10 mM EDTA buffer pH 8. Monoclonal rat anti-human pan-TLE antibody, which recognizes the highly conserved WD-40 domain, has been previously characterized (30) and was graciously provided by S. Stifani (Montreal Neurological Institute, Montréal, Canada). Polyclonal rabbit anti-TLE1 (M-101), which also cross-reacts to a lesser extent with TLE2, 3 and 4, was purchased from Santa Cruz Biotechnology (Santa Cruz, CA). Each microarray section was hybridized with a 1:2 dilution of monoclonal anti-pan-TLE or a 1:20 dilution of M-101 polyclonal anti-TLE1 using a Ventana automated immunostainer (Ventana, AZ) for 30 minutes followed by washing and hybridization with a 1:1000 dilution of HRP-conjugated anti-rat IgG antibody (Abcam, Cambridge, UK). M-101 staining was for comparative purposes also performed manually, using a 1:200 dilution and 4°C overnight incubation. Endogenous peroxidise activity was quenched and antibody visualized by incubation with 3,3'-diaminobenzidine for 10 minutes. TLE immunostaining was graded as "3+" (strong) if greater than 50% of tumor cells per core exhibited intense nuclear staining visible with a 4x low power objective lens, "2+" (moderate) if 10%-50% exhibited intense nuclear staining obvious at low power or greater than 50% nuclear staining well above background when assessed with 10x objective magnification, "1+" (weak) if less than 50% of cells exhibited weak to moderate nuclear staining and "0" (negative) for no visible nuclear staining. Where scores of duplicate cores were discrepant, the higher score was used. Uninterpretable sets of duplicate cores (i.e. no tumor cells, absence of viable cells or folded/lost tissue core) were excluded from analysis. Tumors with a score of 2+ or 3+ on at least one examined tissue microarray core were considered positive for TLE. Sections of each microarray were also stained with hematoxylin and eosin (H&E) using standard methods as an additional histologic reference.

Digital Images

Digital images of immunostained and H&E stained microarrays were acquired using a BLISS imager (Bacus Laboratories, Lombard, IL, USA). A relational database was constructed that correlates scoring and identification information with images of each core. This information is publicly accessible at https://www.gpecimage.ubc.ca/tma/web/viewer.php.

Results

TLE as an immunohistochemical marker

The consistent identification of strong *TLE* expression in synovial sarcoma, from several gene expression profiling studies in different laboratories using different DNA microarray platforms (Table 1) led us to investigate its value as a diagnostic immunohistochemical marker. Two antibodies against TLE1, a monoclonal antibody recognizing an epitope in the C-terminal WD-40 domain, previously shown to work in immunohistochemical applications (30), and a commercially-available polyclonal antibody raised against TLE1, were tested against 693 cases of adult soft tissue tumors including 94 molecularly-validated synovial sarcomas using a tissue microarray format.

Both antibodies gave intense, easy-to-interpret nuclear staining in positive cases. Examples of the four grades of staining, as described in materials and methods, are presented in Figure 1. Original images of tissue cores are available for public review at https://www.gpecimage.ubc.ca/tma/web/viewer.php, and includes H&E, pan-TLE monoclonal and M101 TLE1 polyclonal immunostains on the same (TA-138) tissue microarray for comparative purposes.

The two antibodies (monclonal anti-pan-TLE and M101 polyclonal anti-TLE1) were tested on sequential sections of the TA-138 tissue microarray and found to be almost equivalent (8 discrepancies among 177 cases, Kappa statistic 0.78, $p < 10^{-25}$). Overall, the intensity of optimized staining with M101 was slightly less than with the monoclonal anti-pan-TLE; all discrepancies in scoring (two MPNST, 2 solitary fibrous tumor, 1 schwannoma and 3 synovial sarcomas) between the two antibodies were cases scored positive by pan-TLE and negative by M101. For rigour, tissue microarrays assessing antibody specificity among various sarcomas were assessed with the more sensitive but less specific monoclonal anti-pan-TLE, and the MSKCC arrays, which only contained synovial sarcoma cases, were assessed with the less-sensitive M101. TLE staining results for each tumor type are summarized in Table 2.

Of the 35 bone and soft tissue tumors types with at least 5 cases included in this study, synovial sarcomas were the only type displaying a high proportion of positive TLE staining, with 91/94 (97%) cases exhibiting intense and/or diffuse nuclear staining (i.e. 2+ or 3+; Table 2). TLE staining in a core biopsy of a synovial sarcoma is demonstrated in Figure 2. All cases of biphasic synovial sarcoma exhibited staining in both the epithelial and spindle cell components (Figure 1B), with the epithelial component showing equivalent or stronger intensity. Four cases had the histology of poorly-differentiated synovial sarcoma, and all of these were positive for TLE (three cases scored as 3+, one as 2+). For the synovial sarcoma cases with known *SSX* subtype, all 25 *SYT-SSX1* and all 17 *SYT-SSX2* were positive for TLE. TLE staining was weak (i.e. 1+) in only 3/94 synovial sarcomas while none of the synovial sarcomas had absent (score = 0) staining. TLE staining in a core biopsy of a synovial sarcoma is demonstrated in Figure 2.

In contrast to synovial sarcoma, TLE staining was low to absent in other spindle cell tumors, including those in the differential diagnosis of synovial sarcoma. Solitary fibrous tumor/hemangiopericytomas (6/20) and schwannomas (6/22) were occasionally positive, whereas fibroxanthoma (1/4), clear cell sarcoma (1/7), carcinosarcoma (1/7), high grade chondrosarcoma (1/8), Ewing sarcoma (1/13 cases), MPNST (4/88), gastrointestinal stromal tumor (1/34) and leiomyosarcoma (1/41) were rarely positive for TLE (Table 2). The remaining tumors in this study, including malignant fibrous histiocytoma (MFH, synonymously termed pleomorphic undifferentiated sarcoma), fibrosarcoma and dermatofibrosarcoma protuberans with fibrosarcomatous change, were negative for TLE staining in all examined cases.

Discussion

Distinguishing synovial sarcoma from other spindle cell tumors can present a diagnostic challenge, particularly in those cases that do not exhibit biphasic histology. In these situations immunohistochemical markers can be valuable in confirming the diagnosis of synovial sarcoma. Many attempts have

been made to identify immunomarkers that have high positive predictive value for synovial sarcoma, but to date there have been no markers identified which are both consistently specific and sensitive for this tumor (12, 15, 27). Keratin and/or EMA immuntostains, which are commonly used, are sensitive markers for synovial sarcoma, however their expression is not specific as many tumors, including MPNST, also express epithelial antigens (8, 13, 27).

Gene expression studies in synovial sarcoma have repeatedly shown overexpression of members of the *TLE* family of genes, particularly *TLE1*, in synovial sarcoma. Analysis of this gene expression data has identified *TLE1* as one of the best discriminators for synovial sarcoma when compared to histiologically and/or biologically similar sarcomas such as MPNST or Ewing sarcoma. These data, from multiple groups using different expression profiling platforms, suggest that TLE may be a valuable diagnostic marker for synovial sarcoma.

This study demonstrates that immunohistochemical detection of TLE is not only very highly sensitive for synovial sarcoma, but also specific in the context of other mesenchymal neoplasms. Results are consistent with either a monoclonal antibody recognizing pan-TLE or a commercially available polyclonal antiserum that recognizes TLE1 (and cross-reacts to a lesser extent with TLE2, 3 and 4). We defined positive staining for TLE as moderate to high level staining as described in the materials and methods. Even using stringent criteria, the vast majority of synovial sarcomas (97%) were positive. Other tumors commonly mistaken for synovial sarcoma exhibited lower levels of positive staining for pan-TLE, including schwannomas (27%), Ewing sarcomas (8%), MPNST (5%) and MFH (0%). Notably, TLE expression distinguishes synovial sarcoma from MPNST, a particularly problematic entity in the differential diagnosis, with a high degree of specificity. The majority of the remaining tumor types exhibit low to absent levels of TLE immunostaining, suggesting that TLE is useful in differentiating synovial sarcoma from these tumors. Since a high proportion of cells within most of the synovial sarcoma tissue microarray cores exhibited TLE staining (i.e. 2+ or 3+), high sensitivity on small tissue samples, such as core biopsies, would be seen (Figure 2). Using synovial sarcoma tissue microarrays we have now assessed over 35 established and novel immunohistochemical markers of synovial sarcoma (24), none of which perform as well as TLE.

The prominence of *TLE1* and other components of the Wnt/β-catenin signaling pathway in synovial sarcoma gene expression studies suggest that they may well play an important role in the development of this tumor. The observation that high levels of nuclear-localized β-catenin are a feature of synovial sarcoma (20), and recent experimental data showing that *SYT-SSX* expression leads to accumulation of β-catenin in a nuclear complex that includes SYT-SSX, provides evidence that downstream components of this pathway that mediate its effects on gene transcription are probably important in the pathogenesis of synovial sarcoma (28). The present study demonstrates protein-level correlation of *TLE1* mRNA overexpression in synovial sarcoma. TLE1 competes with activated β-catenin for TCF/LEF transcription factors in the nucleus; TLE1 binding displaces β-catenin to form transcriptionally repressive TLE1-TCF/LEF complexes (4, 9). A recent study demonstrated that β-catenin and SYT-SSX2 interact to potentiate β-catenin-mediated transcription (28), suggesting that TLE1 overexpression may

represent a compensatory response to excessive β-catenin signaling or serve to limit transcriptional activation to certain genes. TLE is also known to associate with other transcription factors, such as HES, where it fulfills a similar role as an adaptor molecule within multiprotein complexes involved in transcriptional repression (6). In this context, TLE may serve to repress genes involved in differentiation and maintain the relatively undifferentiated histopathologic state seen in synovial sarcoma. Further functional studies are required to delineate the role of TLE proteins in synovial sarcoma pathogenesis.

TLE functions to repress transcription via recruitment of histone deacetylase activity (6). Of interest, recent data have shown strong growth inhibition of synovial sarcoma models that were treated with clinically-applicable histone deacetylase inhibitors (17, 18).

In conclusion, TLE1 expression is a consistent and prominent feature of synovial sarcoma whereas it is low to absent in other tumors in the differential diagnosis. Reproducible immunohistochemical staining of TLE1 with negligible background can be obtained with both monoclonal and commercially available polyclonal anti-TLE1 antibodies. TLE1 is a sensitive and specific immunohistochemical marker for synovial sarcoma, performing better than other known immunohistochemical markers, and can significantly aid in the pathologic diagnosis of this tumor.

References

1. Allander SV, Illei PB, Chen Y, et al. Expression profiling of synovial sarcoma by cDNA microarrays: association of ERBB2, IGFBP2, and ELF3 with epithelial differentiation. *Am J Pathol.* 2002;161:1587-1595.

2. Antonescu CR, Kawai A, Leung DH, et al. Strong association of SYT-SSX fusion type and morphologic epithelial differentiation in synovial sarcoma. *Diagn Mol Pathol.* 2000;9:1-8.

3. Baird K, Davis S, Antonescu CR, et al. Gene expression profiling of human sarcomas: insights into sarcoma biology. *Cancer Res.* 2005;65:9226-9235.

4. Brantjes H, Roose J, van De Wetering M, et al. All Tcf HMG box transcription factors interact with Groucho-related co-repressors. *Nucleic Acids Res.* 2001;29:1410-1419.

5. Chang CC, Shidham VB. Molecular genetics of pediatric soft tissue tumors: clinical application. *J Mol Diagn.* 2003;5:143-154.

6. Chen G, Courey AJ. Groucho/TLE family proteins and transcriptional repression. *Gene.* 2000;249:1-16.

7. Chen G, Fernandez J, Mische S, et al. A functional interaction between the histone deacetylase Rpd3 and the corepressor groucho in Drosophila development. *Genes Dev.* 1999;13:2218-2230.

8. Coindre JM, Pelmus M, Hostein I, et al. Should molecular testing be required for diagnosing synovial sarcoma? A prospective study of 204 cases. *Cancer.* 2003;98:2700-2707.

9. Daniels DL, Weis WI. Beta-catenin directly displaces Groucho/TLE repressors from Tcf/Lef in Wnt-mediated transcription activation. *Nat Struct Mol Biol.* 2005;12:364-371.

10. dos Santos NR, de Bruijn DR, van Kessel AG. Molecular mechanisms underlying human synovial sarcoma development. *Genes Chromosomes Cancer.* 2001;30:1-14.

11. Fisher C. Synovial sarcoma. *Ann Diagn Pathol.* 1998;2:401-421.

12. Folpe AL, Schmidt RA, Chapman D, et al. Poorly differentiated synovial sarcoma: immunohistochemical distinction from primitive neuroectodermal tumors and high-grade malignant peripheral nerve sheath tumors. *Am J Surg Pathol.* 1998;22:673-682.

13. Golouh R, Vuzevski V, Bracko M, et al. Synovial sarcoma: a clinicopathological study of 36 cases. *J Surg Oncol.* 1990;45:20-28.

14. Henderson SR, Guiliano D, Presneau N, et al. A molecular map of mesenchymal tumors. *Genome Biol.* 2005;6:R76.

15. Hui P, Li N, Johnson C, et al. HMGA proteins in malignant peripheral nerve sheath tumor and synovial sarcoma: preferential expression of HMGA2 in malignant peripheral nerve sheath tumor. *Mod Pathol.* 2005;18:1519-1526.

16. Husain J, Lo R, Grbavec D, et al. Affinity for the nuclear compartment and expression during cell differentiation implicate phosphorylated Groucho/TLE1 forms of higher molecular mass in nuclear functions. *Biochem J.* 1996;317 (Pt 2):523-531.

17. Ito T, Ouchida M, Morimoto Y, et al. Significant growth suppression of synovial sarcomas by the histone deacetylase inhibitor FK228 in vitro and in vivo. *Cancer Lett.* 2005;224:311-319.

18. Kwan W, Lubieniecka J, Terry J, et al. Effect of depsipeptide (NSC 630176), a histone deacetylase inhibitor, on human synovial sarcoma in vitro. *ASCO 2005 Annual Meeting.* 2005.

19. Ladanyi M. Fusions of the SYT and SSX genes in synovial sarcoma. *Oncogene.* 2001;20:5755-5762.

20. Ladanyi M. Sarcomas with aberrant transcription factors-biology and expression profiling [Connective Tissue Oncology Society Web site]. 2004. Available at: http://www.ctos.org/meeting/2004/program.html. Accessed March 22, 2006.

21. Nagayama S, Katagiri T, Tsunoda T, et al. Genome-wide analysis of gene expression in synovial sarcomas using a cDNA microarray. *Cancer Res.* 2002;62:5859-5866.

22. Ng TL, Gown AM, Barry TS, et al. Nuclear beta-catenin in mesenchymal tumors. *Mod Pathol.* 2005;18:68-74.

23. Nielsen T, Rubin B, Ruttan C, et al. Expression of Groucho/Transducin-like enhancer of split protein distinguishes synovial sarcoma from malignant peripheral nerve sheath tumor [Connective Tissue Oncology Society Web site]. 2005. Available at: http://www.ctos.org/meeting/2005/program.html. Accessed Feb 14, 2006.

24. Nielsen TO, Hsu FD, O'Connell JX, et al. Tissue microarray validation of epidermal growth factor receptor and SALL2 in synovial sarcoma with comparison to tumors of similar histology. *Am J Pathol.* 2003;163:1449-1456.

25. Nielsen TO, West RB, Linn SC, et al. Molecular characterisation of soft tissue tumours: a gene expression study. *Lancet.* 2002;359:1301-1307.

26. Nuthall HN, Husain J, McLarren KW, et al. Role for Hes1-induced phosphorylation in Groucho-mediated transcriptional repression. *Mol Cell Biol.* 2002;22:389-399.

27. Pelmus M, Guillou L, Hostein I, et al. Monophasic fibrous and poorly differentiated synovial sarcoma: immunohistochemical reassessment of 60 t(X;18)(SYT-SSX)-positive cases. *Am J Surg Pathol.* 2002;26:1434-1440.

28. Pretto D, Barco R, Rivera J, et al. The synovial sarcoma translocation protein SYT-SSX2 recruits beta-catenin to the nucleus and associates with it in an active complex. *Oncogene.* 2006.

29. Segal NH, Pavlidis P, Antonescu CR, et al. Classification and subtype prediction of adult soft tissue sarcoma by functional genomics. *Am J Pathol.* 2003;163:691-700.

30. Stifani S, Blaumueller CM, Redhead NJ, et al. Human homologs of a Drosophila Enhancer of split gene product define a novel family of nuclear proteins. *Nat Genet.* 1992;2:119-127.

31. Swingler TE, Bess KL, Yao J, et al. The proline-rich homeodomain protein recruits members of the Groucho/Transducin-like enhancer of split protein family to co-repress transcription in hematopoietic cells. *J Biol Chem.* 2004;279:34938-34947.

32. Terry J, Barry TS, Horsman DE, et al. Fluorescence in situ hybridization for the detection of t(X;18)(p11.2;q11.2) in a synovial sarcoma tissue microarray using a breakapart-style probe. *Diagn Mol Pathol.* 2005;14:77-82.

33. West RB, Harvell J, Linn SC, et al. Apo D in soft tissue tumors: a novel marker for dermatofibrosarcoma protuberans. *Am J Surg Pathol.* 2004;28:1063-1069.

34. Yao J, Liu Y, Lo R, et al. Disrupted development of the cerebral hemispheres in transgenic mice expressing the mammalian Groucho homologue transducin-like-enhancer of split 1 in postmitotic neurons. *Mech Dev.* 2000;93:105-115.

35. Yochum GS, Ayer DE. Pf1, a novel PHD zinc finger protein that links the TLE corepressor to the mSin3A-histone deacetylase complex. *Mol Cell Biol.* 2001;21:4110-4118.

Tables

Study	*TLE1* Rank*	Array Type	Ranking Parameter	SS Cases	Comparison Group
Baird *et al.* Ref #3	5	12600 cDNA spotted	Weighted p-value	16	1 ASPS; 1 CCS; 1 CSa; 5 DFSP; 19 EWS; 7 FSa; 5 GIST; 6 HPCT; 17 LMS; 33 LPS; 38 MFH; 2 MMMT; 5 OSa; 6 BS; 3 MPNST; 6 RMS; 10 NOS
Ladanyi Ref #19	1	22283 probe set Affymetrix U133A	Fold change in expression	46	28 EWS; 28 DSRCT; 23 ARMS; 12 ASPS
Nielsen *et al.* Ref #22	4	42000 cDNA spotted	p-value	13	24 MPNST
Segal *et al.* Ref #28	2	12626 probe set Affymetrix U95A	p-value	5	6 CCS; 5 DDLS; 5 GIST; 8 FSa; 6 LMS; 11 MFH; 3 PLS; 4 RCLS

ARMS: Alveolar rhabdomyosarcoma; ASPS: Alveolar soft parts sarcoma; BS Benign schwannoma; CCS: Clear cell sarcoma; CSa: Chondrosarcoma; DFSP: Dermatofibrosarcoma protuberans; DDLS: Dedifferentiated liposarcoma; DSRCT Desmoplastic small round cell tumor; EWS: Ewing sarcoma; FSa: Fibrosarcoma; GIST: Gastrointestinal stromal tumor; HPCT: Hemangiopericytoma; LMS: Leiomyosarcoma; LPS: Liposarcoma; MFH: Malignant fibrous histiocytoma; MMMT: Malignant Mixed Mullerian tumor; MPNST: Malignant peripheral nerve sheath tumor; NOS: Unclassified sarcoma; OSa: Osteosarcoma; PLS: Pleiomorphic liposarcoma; RCLS: Round-cell liposarcoma; RMS: Rhabdomyosarcoma; SS: Synovial sarcoma

* rank of TLE1 within total gene list when sorted by ability to positively discriminate synovial sarcoma

Table 1 Gene microarray expression profiling studies identify *TLE* as a good discriminator for synovial sarcoma from other sarcomas.

Tumor Type	*n*	*3+*	*2+*	*1+*	*0*	*Total Positive*	*% Positive*
Synovial Sarcoma	94	70	21	3	0	91	**97**
Hemangiopericytoma	5	1	1	1	2	2	**40**
Schwannoma, regular	16	0	5	7	4	5	**31**
Solitary Fibrous Tumor	15	0	4	3	8	4	**27**
Fibroxanthoma	4	0	1	0	3	1	**25**
Schwannoma, cellular	6	0	1	4	1	1	**17**
Carcinosarcoma	7	0	1	2	4	1	**14**
Clear Cell Sarcoma	7	1	0	1	5	1	**14**
Chondrosarcoma, high grade	8	0	1	0	7	1	**13**
Ewing Sarcoma	13	1	0	1	11	1	**8**
GIST	35	0	2	7	26	2	**6**
MPNST	88	1	3	12	72	4	**5**
Leiomyosarcoma	41	1	0	4	36	1	**2**
Angiosarcoma	13	0	0	0	13	0	**0**
Breast Carcinoma	2	0	0	0	2	0	**0**
Chondroblastoma	4	0	0	1	3	0	**0**
Chondromyxoid Fibroma	2	0	0	0	2	0	**0**
Chondrosarcoma, myxoid	7	0	0	2	5	0	**0**
Chondrosarcoma, low grade	23	0	0	0	23	0	**0**
Chondrosarcoma, mesenchymal	2	0	0	0	2	0	**0**
DFSP*	17	0	0	1	16	0	**0**
DSRCT	3	0	0	0	3	0	**0**
Enchondroma	4	0	0	0	4	0	**0**
Endometrial Stromal Sarcoma	11	0	0	1	10	0	**0**
Epithelioid Sarcoma	2	0	0	0	2	0	**0**
Fibromatosis	17	0	0	0	17	0	**0**
Fibrosarcoma	3	0	0	0	3	0	**0**
Giant Cell Tumor, tenosynovial	9	0	0	0	9	0	**0**
Glomous Tumor	7	0	0	1	6	0	**0**
Granular Cell Tumor	8	0	0	0	8	0	**0**
Vascular Tumor **	9	0	0	0	9	0	**0**
Inflammatory Myofibroblastic Tumor	3	0	0	0	3	0	**0**
Kaposi Sarcoma	2	0	0	0	2	0	**0**
Leiomyoma	8	0	0	0	8	0	**0**
Lipoblastomatosis	2	0	0	0	2	0	**0**
Liposarcoma, dedifferentiated	14	0	0	1	13	0	**0**
Liposarcoma, myxoid	4	0	0	1	3	0	**0**
Liposarcoma, pleomorphic	2	0	0	0	2	0	**0**
Liposarcoma, well differentiated	11	0	0	1	10	0	**0**
MFH	56	0	0	5	51	0	**0**
Melanoma	11	0	0	4	7	0	**0**
Myxofibrosarcoma, low grade	5	0	0	0	5	0	**0**
Myxoma	8	0	0	0	8	0	**0**
Myxosarcoma	4	0	0	1	3	0	**0**
Neurofibroma, diffuse	12	0	0	4	8	0	**0**
Neurofibroma, localized	8	0	0	1	7	0	**0**
Neurofibroma, plexiform	24	0	0	5	19	0	**0**
Osteosarcoma	16	0	0	1	15	0	**0**
Perineurioma	4	0	0	0	4	0	**0**
Rhabdomyosarcoma	13	0	0	2	11	0	**0**
Sarcoma, NOS	7	0	0	1	6	0	**0**

DFSP: Dermatofibrosarcoma Protuberans, DSRCT: Desmoplastic Small Round Cell Tumor, GIST: Gastrointestinal Stromal Tumor, MFH: Malignant Fibrous Histiocytoma, MPNST: Malignant Peripheral Nerve Sheath Tumor, NOS: Not Otherwise Sepecified

* Eight of the DFSP cases contained fibrosarcomatous change

** Includes 2 cases of epithelioid hemangioendothelioma, 4 capillary hemangiomas and 3 intramuscular hemangiomas.

Table 2 Summary of TLE immunohistochemistry results.

Figure Legends

Figure 1 TLE immunostaining in representative 0.6 mm cores using pan-TLE antibody. A) 3+ staining in monophasic synovial sarcoma. B) higher power view of 2+ staining in a biphasic synovial sarcoma. C) 1+ staining in MPNST. D) Negative (score = 0) staining in MPNST.

Figure 2 Monoclonal anti-pan-TLE immunostaining of a core needle biopsy, taken from a 6 cm wrist mass in a 49 year-old male. H&E showed a nonpleomorphic spindle cell sarcoma, which was negative for pankeratin, CK7 and EMA by routine diagnostic immunohistochemistry protocols. Subsequent diagnostic FISH assay was positive for a split at the SYT locus, confirming synovial sarcoma 9 days after the TLE immunostaining result. Main image 1.25x, inset 40x. Full biopsy slide available for viewing at https://www.gpecimage.ubc.ca/tma/web/viewer.php

Figure 1

Click here to download high resolution image

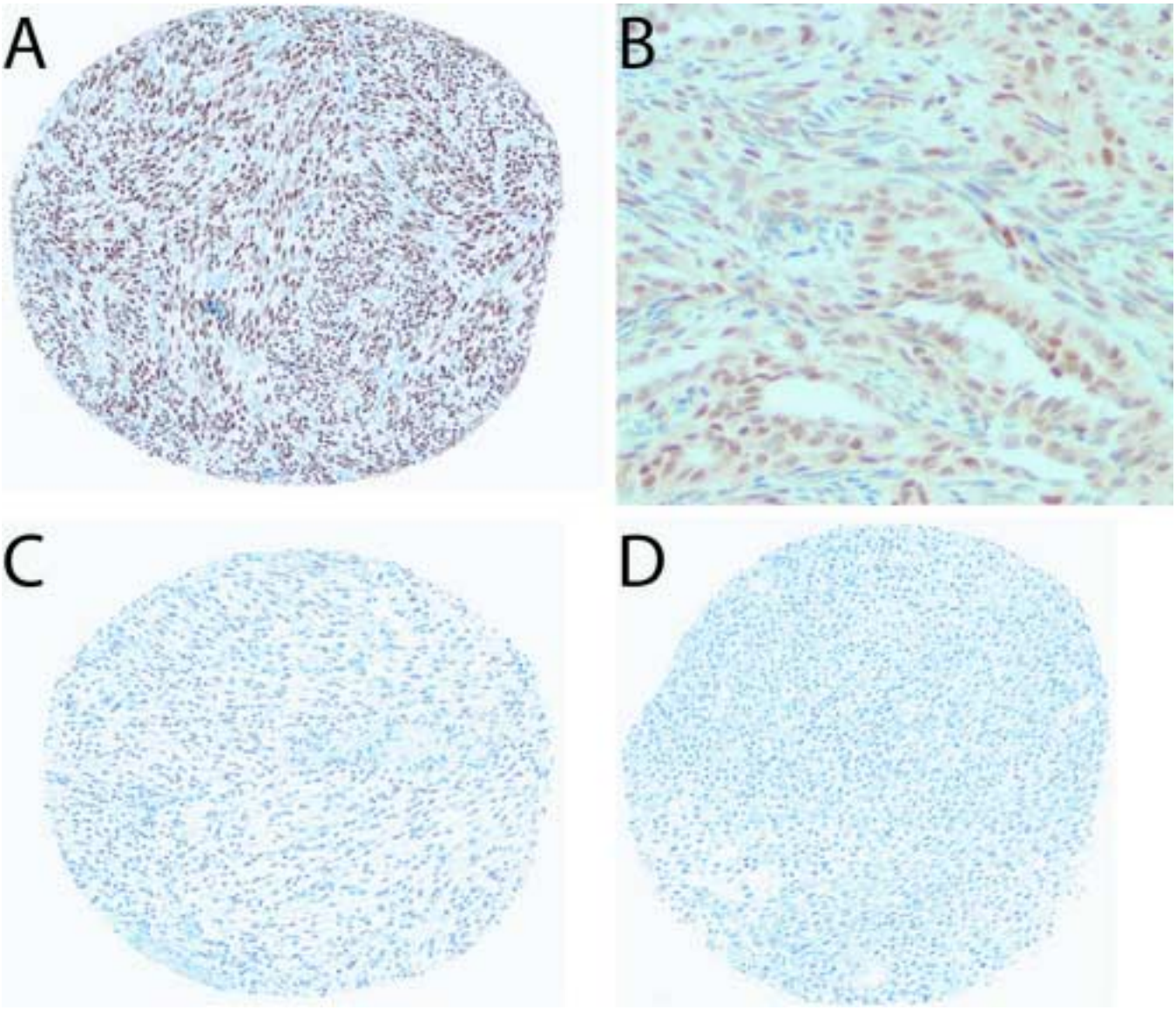

Figure 2

Click here to download high resolution image